

# NONLINEAR CONTROL DESIGN FOR SOLID OXIDE FUEL CELLS

Kandukuri Koteswara Rao

A Thesis Submitted to  
Indian Institute of Technology Hyderabad  
In Partial Fulfillment of the Requirements for  
The Degree of Master of Technology



भारतीय प्रौद्योगिकी संस्थान हैदराबाद  
Indian Institute of Technology Hyderabad

Department of Chemical Engineering

June 2016

## Declaration

I declare that this written submission represents my ideas in my own words, and where ideas or words of others have been included, I have adequately cited and referenced the original sources. I also declare that I have adhered to all principles of academic honesty and integrity and have not misrepresented or fabricated or falsified any idea/data/fact/source in my submission. I understand that any violation of the above will be a cause for disciplinary action by the Institute and can also evoke penal action from the sources that have thus not been properly cited, or from whom proper permission has not been taken when needed.

Koteswara Rao

(Signature)

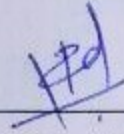
\_\_\_\_\_  
(Kandukuri Koteswara Rao)

CH14Mtech11004

(Roll No.)

## Approval Sheet

This thesis entitled "**Nonlinear Controller Design For Solid Oxide Fuel Cell**" by **Kandukuri Koteswara Rao** is approved for the degree of Master of Technology from IIT Hyderabad.



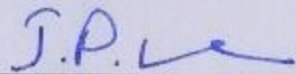
---

(Dr. Ketan P. Detroja) Examiner  
Department of Electrical Engineering, IIT Hyderabad



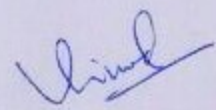
---

(Dr Parag D Pawar) Examiner  
Department of Chemical Engineering, IIT Hyderabad



---

(Dr Phanindra V. Jampana) Adviser  
Department of Chemical Engineering, IIT Hyderabad



---

(Dr Vinod M. Janardhanan) Chairman  
Department of Chemical Engineering, IIT Hyderabad

## Acknowledgements

I would like to thank my parents and family for their endless support which made me stand in IIT Hyderabad. I am very thankful to my guide Dr Phanindra V Jampana for his motivation and encouragement for this project. I also thank my friends and seniors in IIT Hyderabad for their companionship with me. I feel grateful to work with research group (V Goutham Polisetty, K Srikanth and V Santhosh Kumar). I also thank my best friends S Manohar, Ajith Kumar, M Suresh who are going to be memorable part of IIT Hyderabad life. A special thanks to V Goutham Polisetty for his support and encouragement.

## Dedication

I dedicate this thesis to my loving brother Kandukuri Prasad for his support and encouragement through out my life.

## **Abstract**

Ever increasing energy consumption, rising public awareness for environmental protection and higher prices of fossil fuels have motivated many to look for renewable energy sources. SOFC is one of the best alternative energy source but it is a highly nonlinear system. One of the main goals of this research is designing a nonlinear control. In this thesis, non-isothermal model of solid oxide fuel cell has been developed under the general condition of unchoked outlet flow. For isothermal dynamic model of SOFC, a controller based on on full state feedback linearization is designed and compared with controller based on linearization and gain scheduling. Analysis of controllability and observability is also given for the nonlinear isothermal model.

# Contents

Declaration . . . . .	ii
Approval Sheet . . . . .	iii
Acknowledgements . . . . .	iv
Abstract . . . . .	vi
<b>1 INTRODUCTION</b>	<b>1</b>
1.1 Fuel Cell . . . . .	1
1.2 Solid Oxide Fuel Cells . . . . .	3
1.3 Control System Of SOFC . . . . .	3
<b>2 Literature Review</b>	<b>5</b>
2.1 Modeling of SOFC . . . . .	5
2.2 Analysis . . . . .	6
2.3 Controller design . . . . .	6
<b>3 Modeling Of Solid Oxide fuel cell</b>	<b>7</b>
3.1 Lumped Modeling of isothermal SOFC . . . . .	7
3.1.1 Assumptions . . . . .	7
3.1.2 Species Balance . . . . .	7
3.1.3 Electrode Channel Outlet Flow . . . . .	9
3.1.4 Operating conditions . . . . .	9
3.1.5 Anode Channel Outlet Flow Rate . . . . .	10
3.1.6 Cathode Channel Outlet Flow Rate . . . . .	10
3.1.7 Electrochemical model . . . . .	11
3.1.8 Results . . . . .	15
3.2 Modeling of Non-isothermal SOFC . . . . .	18
3.2.1 Energy Balance . . . . .	18
3.2.2 Results . . . . .	18
<b>4 Linear Controller And Gain Scheduling Design</b>	<b>25</b>
4.1 Control Design by Approximate Linearlization . . . . .	26
4.1.1 Approximate Linear Control Design For SOFC . . . . .	28
4.1.2 Result . . . . .	29
4.2 Control Design Using Gain Scheduling . . . . .	31
4.2.1 Results . . . . .	32

<b>5</b>	<b>Nonlinear Controllability And Observability</b>	<b>34</b>
5.1	Controllability . . . . .	34
5.1.1	Controllability For Nonlinear System . . . . .	34
5.1.2	Controllability of Nonlinear Systems Using Differential Geometry . . . . .	35
5.1.3	Controllability of Isothermal SOFC Using Differential Geometry . . . . .	35
5.2	Observability . . . . .	36
5.2.1	Observability For Nonlinear Systems . . . . .	36
5.2.2	Observability For Nonlinear System Using Differential Geometry . . . . .	36
5.2.3	Observability For Isothermal SOFC Using Differential Geometry . . . . .	37
<b>6</b>	<b>Feedback Linearization Controller Design</b>	<b>38</b>
6.1	Full-State Feedback Linearization . . . . .	38
6.2	Full state feedback linearization controller design for SOFC . . . . .	40
6.3	Results . . . . .	41
6.4	Comparison Between Feedback Linearization And Approximate Linearization Control Performance . . . . .	42
<b>7</b>	<b>Conclusions And Future Work</b>	<b>45</b>



# Chapter 1

## INTRODUCTION

### 1.1 Fuel Cell

The first fuel cell was invented by William Grove. Fuel cell is an electrochemical device which can directly convert chemical energy into electrical energy through an electrochemical process. The main difference between chemical and electrochemical reactions is that while electrochemical reactions involve the transfer of charge between an electrode and a chemical species, in a chemical reaction, charge transfer occurs directly between two chemical species without liberation of free electrons.

The overall reaction of the fuel cell is based on simple water formation reaction between hydrogen and oxygen.



In the direct reaction there is no charge transfer but in an electrochemical reaction, the reactants hydrogen (fuel) and oxygen (air) are taken separately and given enough activation energy so that hydrogen releases two electrons which are accepted by oxygen. The electron rich electrode which is on the side of hydrogen is called as Anode and the electron deficient electrode which is on the oxygen side is called as cathode. There exists a potential difference between anode and cathode.

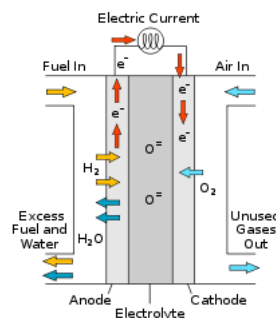


Figure 1.1: SOFC

The potential difference is used to drive a current from anode to cathode using an external conductor (wire). Oxygen ions pass through the ceramic electrolyte to the hydrogen side to complete

the reaction and the circuit. The main difference between a traditional battery is that the fuel cell is a continuous process - a current can be extracted as long as the reactants are supplied. The important steps involved in producing electricity in a fuel cell are reactant delivery into the fuel cell, electrochemical reaction, ionic conduction through the electrolyte, electron conduction through external circuit and product removal from the fuel cell.

### Types of fuel cells

There are five major types of fuel cells. Differentiated by type of electrolyte used [1].

1. Phosphoric Acid Fuel Cell (PAFC)
2. Polymer Electrolyte Membrane Fuel Cell (PEMFC)
3. Alkaline Fuel Cell (AFC)
4. Molten Carbonate Fuel Cell (MCFC)
5. Solid Oxide Fuel Cell (SOFC)

Fuel cell type	Electrolyte	Temperature	Efficiency	Charge Carrier
PAFC	Phosphoric acid	150 – 200°C	40	$H^+$
PEMFC	Thin polymer membrane	50 – 100°C	30 – 60	$H^+$
AFC	Caustic potash solution	90 – 100°C	60	$OH^-$
MCFC	Molten carbonate	600 – 700°C	50 – 60	$CO_3^{2-}$
SOFC	Ceramic	600 – 1000°C	50 – 60	$O^{2-}$

Table 1.1: Types of Fuel Cells. Parameter values are taken from [1]

### Advantages of fuel cells

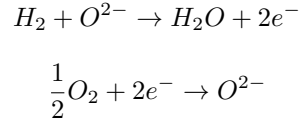
- Fuel cells produce electricity directly from chemical energy, they are often more efficient combustion engines
- As long as fuel is supplied a current can be extracted
- Components of fuel cell are can be all solid state, mechanically there are no moving parts. This yields the potential for high reliable long lasting system.
- Undesired products such as  $NO_x$ ,  $SO_x$ , particularly emissions are virtually zero.
- Easy to scale up from 1 watt to 1 mega watt

### Disadvantages of fuel cells

- Cost is a major barrier to fuel cell implementation.
- Power density is significant limitation
- Operating temperature is also one of the limitations.
- Fluctuation in output voltage whenever there is small change in operating conditions.

## 1.2 Solid Oxide Fuel Cells

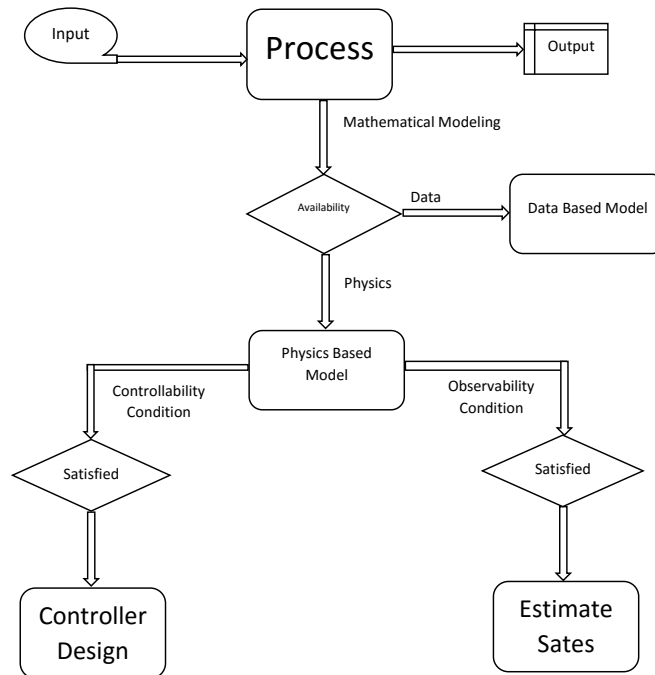
Solid oxide fuel cells operate at high temperatures, usually in the range of  $600^{\circ}C$  to  $1000^{\circ}C$  and employ a ceramic electrolyte. The most common electrolyte is Yttria-stabilized zirconia. Oxygen ions  $O^{2-}$  are the charge carriers. The electrochemical reaction is given by



SOFCs are known for their higher electrical efficiency of about 50-60 percentage compared to other types of fuel cells and are considered very suitable in stationary power generation applications.

## 1.3 Control System Of SOFC

### Overview of Control System



The purpose of a controller is to make the plant behave in a desired manner. Power generation plants need to have very specific and fixed desired output value with unnoticeable fluctuations. As SOFC is a highly nonlinear plant, a non-linear controller might give better performance. The control technology is critical in its development and is an important factor for commercializing the SOFC.

A reliable and accurate control oriented model is of great importance to understanding the dynamic characteristics of the SOFC. Modeling of a plant can be done in two ways, one is data based modeling and the second one is physics based modeling. Collecting SOFC experimental data

is difficult and expensive. This is probably the reason why most of the researchers used physics based models for control of SOFC.

After developing a dynamic model, a study on of stability, controllability and observability needs to be performed. One of the ways for checking these properties for a nonlinear model is through linearization at operating points. In approximate linearization, higher order terms in Taylor expansions are truncated. Dynamics of linear and nonlinear models will be similar close to the operating point. A controller can be designed for the linear model at that operating point. If the nonlinear plant is operated away from this operating point, linear controllers do not give good performance.

Using differential geometry, controllability and observability, can be directly verified for the nonlinear system. There exist many controllers in the existing literature [2], [3] for SOFC. In these designs, assumptions are made that state equations are linear. With the help of exact linearization, the nonlinear state equations system can be transformed into an equivalent linear state space system.

There exist two types of feedback linearization 1) full state feedback linearization and 2) input-output linearization [4], [5]. For full state feedback linearization, the system should be controllable and observable. In this thesis controller design is obtained using full-state feedback linearization for controlling pressure dynamics such that we will get desirable voltage.

# Chapter 2

## Literature Review

Solid oxide fuel cells have been a key area of academic research interest over the past decade due to their high electrical efficiency, fuel flexibility, and high quality waste heat. Modeling of SOFC, analysis, estimation of states and controller design are major steps of the control system.

### 2.1 Modeling of SOFC

Control techniques applied to the SOFC based on process models, require simple and accurate differential and algebraic equations that should represent the SOFC dynamic response characteristics. So far, there have been many publications [6], [7], [8], [9] on the dynamic models of the SOFC. [7] include spatial variation of fuel cell parameters, and [8] include mass and heat transfer but it is very difficult to study control performance of fuel cell with such detailed dynamics.

Some researchers introduced zero-dimensional, lumped dynamic models [7], [9], [10], [11] which are suitable for designing control systems. Operating state parameters in SOFC are partial pressures of species and temperature. Many researchers designed mathematical dynamic modeling of SOFC at constant temperature for explicit study of pressure dynamics [9], [10].

From control design point of view, the output from the fuel cell is current density or voltage. Operating at high pressure gives high current density, but it may damage the electrolyte and product removal becomes difficult. There have been many studies on lumped models for fuel cells at high operating pressure [7], [9]. Most of the researchers who carried out lumped modeling in the past considered the choking flow assumption in determining outlet flow rate of gas through an orifice at the exit of electrode channels [7]. The flow is said to be choked if the ratio of downstream pressure to upstream pressure is less than or equal to 0.529 [12]. Whether flow is choked or not also depends on other parameters like inlet flow rate, orifice cross sectional area, channel area and current withdrawn.

If outlet flow of species is choked then outlet flow rate is proportional to inside partial pressure species [7]. For low operating pressure conditions the resulting flow is unchoked at outlet. Mathematical expression for unchoked outlet flow rate is nonlinear function of inside partial pressures and temperature. It can be derived using compressible Bernoulli equation [13].

Including temperature variations in dynamic model of SOFC at high operating pressures is presented in [7]. One of the research groups has done dynamic model SOFC for choked flow [10] but they consider only pressure dynamics and stack temperature is constant. One of the challenges is

to develop the dynamic modeling of SOFC for low operating pressures with temperature variations.

## 2.2 Analysis

Study of controllability and observability for linear dynamic models or state space models are given in [14]. For nonlinear models, such analysis by linearization of nonlinear model at some operating point is presented in [15]. The nonlinear model considered in this thesis is described by

$$\dot{x} = f(x) + g(x)u;$$

$$y = h(x);$$

Controllability and observability analysis can be done using differential geometry [16]. Isothermal SOFC dynamic model for low operating pressure can be written in the form which is mentioned above. In this thesis differential geometry based techniques are applied to SOFC model for analysis of controllability and observability.

## 2.3 Controller design

There are many control strategies in literature for nonlinear systems. Isothermal SOFC is a highly nonlinear system and there exist a few optimal control techniques applied to nonlinear SOFC [2]. [17] has applied feedback linearization controller to Proton exchange membrane fuel cell. In this thesis, feedback linearization is applied to a dynamic model of isothermal SOFC.

# Chapter 3

## Modeling Of Solid Oxide fuel cell

### 3.1 Lumped Modeling of isothermal SOFC

The dynamic model is especially beneficial for control study in the development stage of SOFC. Lumped model is the simplest way to model the dynamics, where we neglect the spatial variation and consider only the changes with time.

#### 3.1.1 Assumptions

The following are the assumptions of lumped model

- The gases are assumed to be ideal.
- Unchoked flow assumption is considered while modeling the outlet flow through orifice at exit of gas channels.
- Temperature is assumed to be uniform in the entire stack.
- Ideal mixing of gases is considered.

#### 3.1.2 Species Balance

The fuel and air are supplied through anode and cathode channels respectively. Species balance is carried out separately by applying law of conservation of mass.

##### Species balance in an anode channel

Anode channel contains two species :  $H_2$  and  $H_2O$ . First we write species balance for  $H_2$  as

$$\frac{dn_{H_2}}{dt} = \dot{n}_{H_2}^{in} - \dot{n}_{H_2}^{out} + \dot{n}_{H_2}^r$$

where

- $n_{H_2}$  is molar flow rate of  $H_2$  in the stack, it can be expressed as  $n_{H_2} = (P_{H_2}V_{an})/(RT_s)$  using Ideal gas law, here  $V_{an}$  is the volume of anode channel,  $P_{H_2}$  is partial pressure of  $H_2$  in the stack,  $R$  is Universal Gas Constant and  $T_s$  is temperature of the stack.

- $\dot{n}_{H_2}^{in}$  is inlet molar flow rate of  $H_2$ , This is used as an input to the control system.
- $\dot{n}_{H_2}^r$  is reactive molar flow rate of  $H_2$ , it can be expressed as  $\dot{n}_{H_2}^r = -2K_r I$ , where  $K_r = \frac{N_o}{4F}$ ,  $I$  is stack current,  $N_o$  is number of cells connected in series in stack and  $F$  is Faraday's Constant.
- $\dot{n}_{H_2}^{out}$  is outlet molar flow rate of  $H_2$ , it is proportional to the  $P_{H_2}$  when outlet molar flow is choked at the orifice [7]. The derivation for general unchoked outlet molar flow is given in the next subsections.

Using the above, the species balance of  $H_2$  can be written as

$$\frac{dP_{H_2}}{dt} = \frac{RT_s}{V_{an}} (\dot{n}_{H_2}^{in} - \dot{n}_{H_2}^{out} - 2K_r I)$$

Similarly the species balance equation for  $H_2O$  is

$$\frac{dP_{H_2O}}{dt} = \frac{RT_s}{V_{an}} (\dot{n}_{H_2O}^{in} - \dot{n}_{H_2O}^{out} + 2K_r I)$$

### Species balance in a cathode channel

Cathode channel has two species :  $O_2$  and  $N_2$ . First we write species balance for  $O_2$  as

$$\frac{dn_{O_2}}{dt} = \dot{n}_{O_2}^{in} - \dot{n}_{O_2}^{out} + \dot{n}_{O_2}^r$$

where

1.  $n_{O_2}$  is molar flow rate of  $O_2$  in the stack, it can be expressed as  $n_{O_2} = (P_{O_2} V_{cat}) / (RT_s)$  using Ideal gas law, here  $V_{cat}$  is the volume of cathode channel,  $P_{O_2}$  is partial pressure of  $O_2$  in the stack.
2.  $\dot{n}_{O_2}^{in}$  is inlet molar flow rate of  $O_2$ , we should give optimal inlet molar flow rate to maintain desirable operating conditions to get desirable output for this we need to have good control system.
3.  $\dot{n}_{O_2}^r$  is reactive molar flow rate of  $O_2$ , it can be expressed as  $\dot{n}_{O_2}^r = -K_r I$ .
4.  $\dot{n}_{O_2}^{out}$  is outlet molar flow rate of  $O_2$ , it is proportional to the  $P_{O_2}$  when outlet molar flow is choked at the orifice [7].

Therefore, the species balance of  $O_2$  is

$$\frac{dP_{O_2}}{dt} = \frac{RT_s}{V_{cat}} (\dot{n}_{O_2}^{in} - \dot{n}_{O_2}^{out} - K_r I)$$

Similarly the species balance equation for  $N_2$  is

$$\frac{dP_{N_2}}{dt} = \frac{RT_s}{V_{cat}} (\dot{n}_{N_2}^{in} - \dot{n}_{N_2}^{out})$$



### 3.1.3 Electrode Channel Outlet Flow

To obtain outlet flow rate in an electrode channel, we consider unchoked outlet flow and assume that the flow of gaseous mixture to be adiabatic through the orifice. The Bernoulli's equation for compressible flow [18] is

$$\frac{v_1^2}{2} + \left(\frac{\gamma}{\gamma-1}\right) \frac{P_1}{\rho_1} = \frac{v_2^2}{2} + \left(\frac{\gamma}{\gamma-1}\right) \frac{P_2}{\rho_2} \quad (3.1)$$

Continuity equation for compressible flow is  $\rho_1 v_1 A_1 = \rho_2 v_2 A_2$  where,  $P_1$ ,  $P_2$  are upstream, downstream pressures and  $\rho_1$ ,  $\rho_2$  are upstream, downstream densities at orifice,  $\gamma$  is ratio of specific heats.  $A_1$ ,  $A_2$  is cross section area of manifold and orifice. Further simplifying the above equations we take  $\beta = D_2/D_1$ ,  $r = P_2/P_1$  and substitute  $v_1 = v_2 \beta^2 r^{1/\gamma}$  in equation (3.1) to obtain

$$v_2^2 = \frac{P_1}{\rho_1} \left(\frac{2\gamma}{\gamma-1}\right) \left(1 - r^{\frac{\gamma-1}{\gamma}}\right) \left(\frac{1}{1 - r^{\frac{2}{\gamma}} \beta^4}\right) \quad (3.2)$$

Dividing and multiplying by  $(P_1 - P_2)$ , we get

$$v_2 = \sqrt{\frac{2}{\rho_1} \left(\frac{\gamma}{\gamma-1}\right) \left(\frac{1 - r^{\frac{\gamma-1}{\gamma}}}{1 - r}\right) \left(\frac{(P_1 - P_2)}{1 - r^{\frac{2}{\gamma}} \beta^4}\right)} \quad (3.3)$$

Finally, the mass flow rate out from orifice is expressed as

$$\dot{m}_{out} = C_d \rho_2 A_2 \sqrt{\frac{2}{\rho_1} \left(\frac{\gamma}{\gamma-1}\right) \left(\frac{1 - r^{\frac{\gamma-1}{\gamma}}}{1 - r}\right) \left(\frac{(P_1 - P_2)}{1 - r^{\frac{2}{\gamma}} \beta^4}\right)}$$

$C_d$  is Discharge Coefficient of orifice and is used to measure the ratio of the actual discharge to the theoretical discharge [19]. Let  $C = \frac{C_d}{\sqrt{1-\beta^4}}$  and

$$Y = \sqrt{r^{\frac{2}{\gamma}} \left(\frac{\gamma}{\gamma-1}\right) \left(\frac{1 - r^{\frac{\gamma-1}{\gamma}}}{1 - r}\right) \frac{1 - \beta^4}{1 - r^{\frac{2}{\gamma}} \beta^4}}$$

Using these the mass flow rate out becomes

$$\dot{m}_{out} = CY A_2 \sqrt{2\rho_1(P_1 - P_2)}$$

### 3.1.4 Operating conditions

The International Energy Agency (IEA) conducted a fuel cell stack modeling exercise that involved seven European countries and Japan [6]. The operating conditions used are

- Operating pressure = 1 Bar.
- Operating temperature = 1173.15 K.

In this thesis we assume that operating pressure is slightly higher than the atmospheric pressure and fuel cell outlet is open to the atmosphere. Therefore the difference between the operating pressure

and the outside pressure is small. We note that  $r \approx 1$ . If we apply limit  $r \rightarrow 1$  in the above equation for  $Y$ , we obtain

$$\lim_{r \rightarrow 1} Y = \lim_{r \rightarrow 1} \sqrt{r^{\frac{2}{\gamma}} \left( \frac{\gamma}{\gamma-1} \right) \left( \frac{1-r^{\frac{\gamma-1}{\gamma}}}{1-r} \right) \frac{1-\beta^4}{1-r^{\frac{2}{\gamma}}\beta^4}} = 1$$

(by applying *L'Hopital's* rule) and hence mass flow rate out can be expressed as

$$\dot{m}_{out} \approx CA_2 \sqrt{2\rho_1(P_1 - P_2)} \quad (3.4)$$

### 3.1.5 Anode Channel Outlet Flow Rate

Using above mentioned general expression for electrode mass outlet flow rate we need to derive molar outlet flow rate of each species in the anode channel. Mass flow rate out through the anode channel is calculated as

$$\dot{m}_{anode}^{out} = CA_a \sqrt{2\rho_a(P_{H_2} + P_{H_2O} - P_{atm})} \quad (3.5)$$

where  $P_1 = (P_{H_2} + P_{H_2O})$ ,  $P_2 = P_{atm}$ ,  $A_a$  is anode side orifice cross sectional area and  $\rho_a$  is the density of gaseous mixture in anode channel which can be expressed as  $\rho_a = \frac{P_1 M_a}{RT}$ .  $M_a$  is the average molecular weight of gas in the anode channel which can be calculated as

$$M_a = \frac{P_{H_2} M_{H_2} + P_{H_2O} M_{H_2O}}{P_{H_2} + P_{H_2O}} \quad (3.6)$$

where  $P_{H_2}$  and  $P_{H_2O}$  are partial pressures of  $H_2$  and  $H_2O$  inside the fuel cell,  $M_{H_2}$  and  $M_{H_2O}$  are molecular weights of  $H_2$  and  $H_2O$ . Molar flow rate out for the anode side is  $\dot{n}_a^{out} = \dot{m}_{anode}^{out}/M_a$ . Substituting the above equations (3.5), (3.6) and simplifying we obtain

$$\dot{n}_{anode}^{out} = CA_a (P_{H_2} + P_{H_2O}) \sqrt{\frac{2(P_{H_2} + P_{H_2O} - P_{atm})}{RT_s (P_{H_2} M_{H_2} + P_{H_2O} M_{H_2O})}} \quad (3.7)$$

Molar flow rate out for each species in an anode channel can then be calculated as

$$\dot{n}_{H_2}^{out} = \frac{P_{H_2}}{P_{H_2} + P_{H_2O}} \dot{n}_{anode}^{out} = CA_a P_{H_2} \sqrt{\frac{2(P_{H_2} + P_{H_2O} - P_{atm})}{RT_s (P_{H_2} M_{H_2} + P_{H_2O} M_{H_2O})}}$$

$$\dot{n}_{H_2O}^{out} = \frac{P_{H_2O}}{P_{H_2} + P_{H_2O}} \dot{n}_{anode}^{out} = CA_a P_{H_2O} \sqrt{\frac{2(P_{H_2} + P_{H_2O} - P_{atm})}{RT_s (P_{H_2} M_{H_2} + P_{H_2O} M_{H_2O})}}$$

### 3.1.6 Cathode Channel Outlet Flow Rate

Mass flow rate out through the cathode channel can be calculated as

$$\dot{m}_{cathode}^{out} = CA_c \sqrt{2\rho_c(P_{O_2} + P_{N_2} - P_{atm})} \quad (3.8)$$

where  $P_1 = (P_{O_2} + P_{N_2})$ ,  $P_2 = P_{atm}$ ,  $A_c$  is the cathode side orifice cross sectional area and  $\rho_c$  is the density of gaseous mixture in the cathode channel which can be expressed as  $\rho_c = \frac{P_1 M_c}{RT}$ .  $M_c$  is the

average molecular weight of gas in the cathode channel which is calculated as

$$M_c = \frac{P_{O_2}M_{O_2} + P_{N_2}M_{N_2}}{P_{O_2} + P_{N_2}} \quad (3.9)$$

where  $P_{O_2}$  and  $P_{N_2}$  are partial pressures of  $O_2$  and  $N_2$  inside the fuel cell,  $M_{H_2}$  and  $M_{H_2O}$  are molecular weights of  $O_2$  and  $N_2$ . Molar flow rate out for cathode side is  $\dot{n}_c^{out} = \dot{m}_{cathode}^{out}/M_c$ . Substituting the above equations and simplifying we get

$$\dot{n}_c^{out} = CA_c(P_{O_2} + P_{N_2})\sqrt{\frac{2(P_{O_2} + P_{N_2} - P_{atm})}{RT_s(P_{O_2}M_{O_2} + P_{N_2}M_{N_2})}} \quad (3.10)$$

Molar flow rate out for each species in cathode channel is

$$\dot{n}_{O_2}^{out} = \frac{P_{O_2}}{P_{O_2} + P_{N_2}}\dot{n}_{anode}^{out} = \dot{n}_{O_2}^{out} = CA_cP_{O_2}\sqrt{\frac{2(P_{O_2} + P_{N_2} - P_{atm})}{RT_s(P_{O_2}M_{O_2} + P_{N_2}M_{N_2})}}$$

$$\dot{n}_{N_2}^{out} = \frac{P_{N_2}}{P_{O_2} + P_{N_2}}\dot{n}_{anode}^{out} = CA_cP_{N_2}\sqrt{\frac{2(P_{O_2} + P_{N_2} - P_{atm})}{RT_s(P_{O_2}M_{O_2} + P_{N_2}M_{N_2})}}$$

### 3.1.7 Electrochemical model

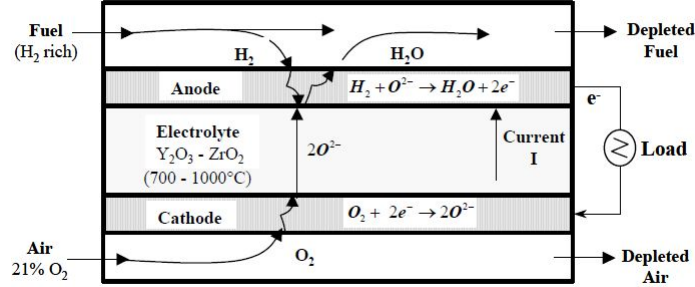


Figure 3.1: Electrochemical Processes within a solid oxide fuel cell [6]

The electrochemical processes taking place in the solid oxide fuel cell are as illustrated in Figure 3.1. As shown in the figure, the potential of the electrons released at the anode is smaller than that of the electrons taken up by the oxygen at the cathode. The cell delivers net power as electricity. The maximum theoretical work for a steady-flow open process is given by the change in molar Gibbs free energy of the process  $\Delta G$ . The electrical work done by a fuel cell is given by the amount of charge that flows from the cell multiplied by the driving force that causes it to flow i.e., the potential difference of the cell [6]. This can be expressed as,  $W_{max} = -\Delta G = n_eFE$ . Here  $n_e$  is the number of moles of electrons transferred in the overall reaction. The maximum potential difference given by open circuit voltage.

## Open Circuit Voltage

Thermodynamic potential or the reversible cell voltage is the maximum voltage attained by solid oxide fuel cell at thermal equilibrium. It is given by Nernst Equation (including temperature effects) [1] as below

$$V_0 = N_0 \left[ \Delta E_0 + \frac{\Delta s}{nF}(T - T_o) + \frac{RT_s}{2F} \log \left( \frac{P_{H_2} P_{O_2}^{0.5}}{P_{H_2O} P_{atm}^{0.5}} \right) \right]$$

where  $N_0$  is the total number of cells in the stack,  $\Delta E_0$  is standard cell potential given by  $\Delta E_0 = -\frac{\Delta G_0}{2F}$  and  $\Delta s$  is the change in entropy of the reaction. The values for  $\Delta s$ ,  $\Delta G_0$  are taken from [20]. In real solid oxide fuel cell operation we experience loss in efficiency due to other effects. Temperature, pressure, gas composition, conductivity of materials, amount of the current extracted from SOFC, fuel and reactant utilization influence their performance. These operating variables affect the magnitude of the irreversible voltage losses. The losses, when expressed in terms of voltages, are called polarization. There are three main types of polarizations

- 1 Ohmic Polarization ( $\eta_{ohm}$ ).
- 2 Activation Polarization ( $\eta_{act}$ ).
- 3 Concentration Polarization ( $\eta_{con}$ ).

## Stack Voltage

In modeling the stack voltage we consider all polarizations mentioned above. The stack voltage is given by the following equation

$$V_s = N_o (V_0 - \eta_{ohm} - \eta_{act} - \eta_{con}) \quad (3.11)$$

## Ohmic Polarization

Voltage which is lost due to resistance to flow of ions through electrolyte is known as Ohmic polarization. Ohmic Loss is given by [11]  $V_{ohm} = IR$  where  $I$  is the current (A) and  $R$  is the ohmic resistance ( $\Omega$ ).  $R$  is given by

$$R = 0.2 \exp \left[ -2870 \left( \frac{1}{1196.15} - \frac{1}{T} \right) \right]$$

## Activation Polarization

Activation loss is the extra potential necessary to overcome the energy barrier of the rate determining step of the reaction to a value such that electrode reaction proceeds at desired reaction rate. We consider cathode activation loss here as the Anode activation is relatively negligible. Activation polarization expression is given by [1]

$$\eta_{act} = \frac{2RT_s}{nF} \sinh^{-1} \left( \frac{i}{2i_o} \right)$$

where  $i_o$  is exchange current density [10].

## Concentration Polarization

The concentration loss is due to limited rate at which reactant concentrations can change, which limits the rate at which the reactants can be transported to the electrode surfaces. During the fuel cell operation, there is a slight reduction in the concentration of the reactants in the region of the electrode, as the reactant is extracted. The extent of this change in concentration will depend on the current being taken from the fuel cell [20]. The concentration loss is given by

$$\eta_{conc} = -\frac{RT}{4F} \ln \left( 1 - \frac{j}{j_L} \right)$$

where  $j_L$  is limiting current density.

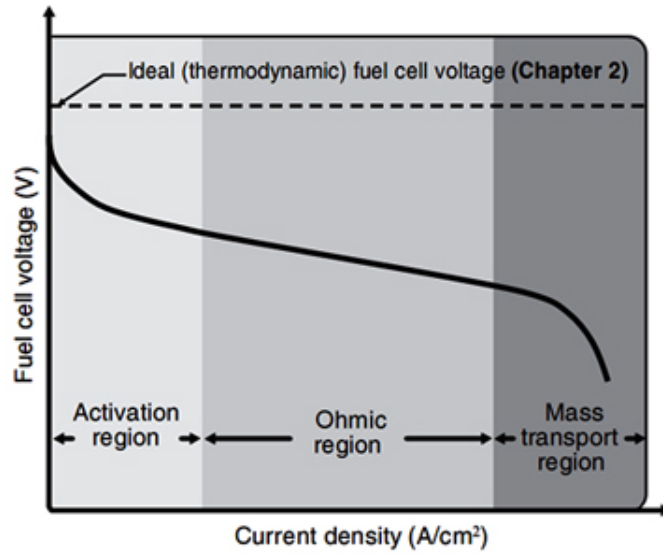


Figure 3.2: Overall effect of polarization on cell voltage performance [1]

As shown in the figure above at very low current density activation polarization is dominant, at intermediate current densities Ohmic polarization is dominant, at high current density concentration polarization is dominant.

The complete list of parameter values used in the model are given below.

Parameter	Value	Units
No of cells ( $N_o$ )	384	
Anode channel c/s area $A_{an}$	0.0025	$m^2$
Cathode channel c/s area $A_{cat}$	0.0025	$m^2$
Cell Area	0.1	$m^2$
Coefficient of Discharge $C_d$	0.75	
Ambient Pressure $P_{atm}$	101325	$Pa$
$C_p$ of stack	470	$J/kgK$
Temperature( $T_s$ )	1273.15	$K$
Inlet Fuel flow rate	2	$mol/s$
Inlet Air flow rate	5	$mol/s$
Inlet $H_2$ mole fraction in fuel	1	
Inlet Temperature	1073.15	$^{\circ}C$
Anode Volume( $V_a$ )	0.2	$m^3$
Cathode Volume( $V_c$ )	0.2	$m^3$
Molecular Weight of ( $H_2$ )	$2.016 * 10^{-03}$	$kg/mole$
Molecular Weight of ( $H_2O$ )	$18.016 * 10^{-03}$	$kg/mole$
Molecular Weight of ( $O_2$ )	$28.014 * 10^{-03}$	$kg/mole$
Molecular Weight of ( $H_2$ )	$31.998 * 10^{-03}$	$kg/mole$
Exchange Current Density ( $j_o$ )	1500	$\frac{A}{m^2}$
Limiting Current Density ( $j_L$ )	10000	$\frac{A}{m^2}$
$\Delta G_o$	$-194.2e3$	$J/mol$
$\Delta s$	$-54.9$	$J/mol$
$\Delta G_o$	$-194.2e3$	$J/mol$

Table 3.1: Parameter Values. Some of the parameter values are taken from [10].

### Schematic Simulink Model of Isothermal SOFC

The above discussed lumped model of isothermal SOFC with unchoked flow is modeled in MATLAB Simulink as shown below.

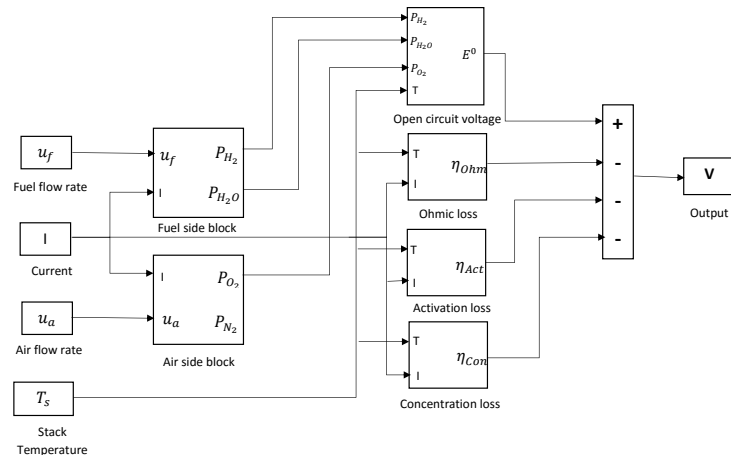


Figure 3.3: Schematic simulink model of isothermal SOFC

### 3.1.8 Results

The above lumped model of isothermal SOFC has been simulated in MATLAB Simulink . It can be observed that V-I curve from the simulation follows same trend as theoretical V-I curve given by [1]. For a step up in fuel flow rate from 2 to 2.5 mole/sec and step up in current from 400 to 500A, the results obtained are similar to [10].

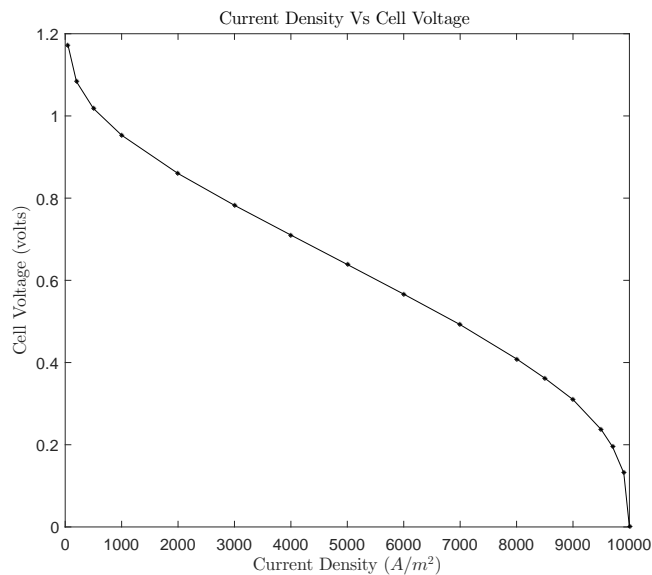


Figure 3.4: V-I Curve for Isothermal SOFC at fuel flow rate is 2 mole/sec, Air flow rate is 5 mole/sec.

Figure 3.3 shows the steady state voltage output from the lumped model at various currents. It

can be seen that voltage decreases with current density in the simulated range.

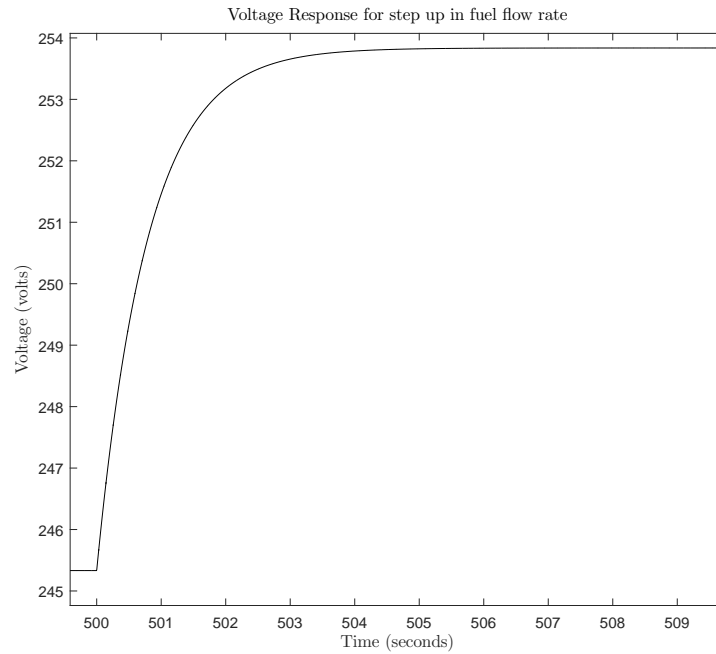


Figure 3.5: Step in fuel flow rate from 2 to 2.5 *mole/sec* at air flow rate is 5 *mole/sec* and current 500A.

Figure 3.4 illustrates the dynamics of voltage when there is step up fuel flow rate from 2 mole/sec to 2.5 mole/sec. Steady state voltage increases because of increase in reactant pressure inside the fuel cell and it is also observed that the dynamics is very fast.



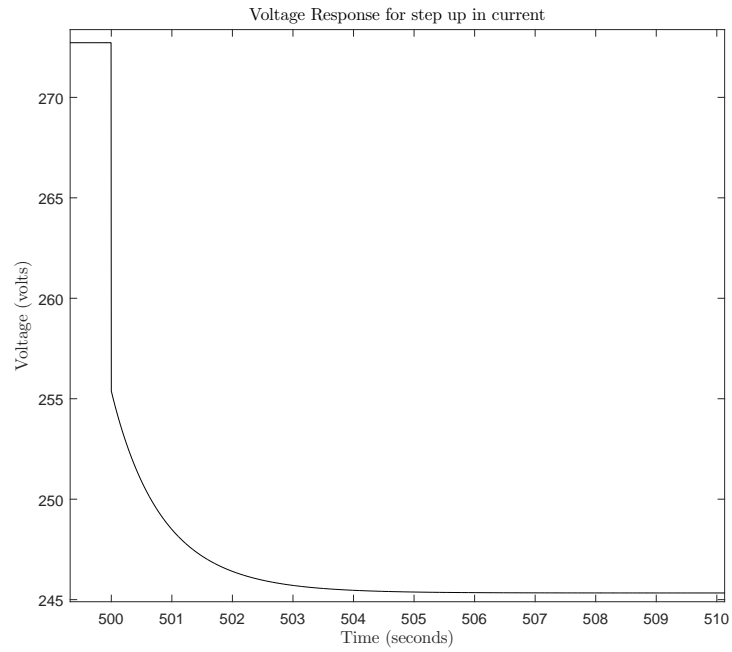


Figure 3.6: Step in current from 400 to 500A at fuel flow rate is 2 *mole/sec*, Air flow rate is 5 *mole/sec*.

Figure 3.5 shows that the dynamics of voltage when a step up in current from 400 to 500A is applied. Steady state voltage decreases mainly due to increase in activation loss and ohmic loss.

## 3.2 Modeling of Non-isothermal SOFC

In previous section we built the dynamic lumped model of SOFC by assuming that stack temperature is constant. Practically, as temperature dynamics is very slow temperature will take more time to reach steady state. Species balance and electrochemical equations for dynamic lumped model of non-isothermal SOFC are same as mentioned in the above isothermal SOFC model. However, stack temperature is not constant. For calculating stack temperature dynamics we use the energy balance.

### 3.2.1 Energy Balance

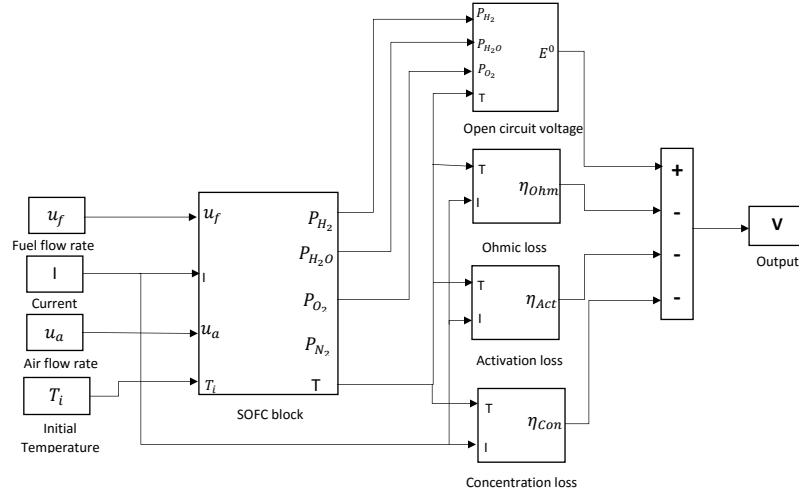
In the lumped stack modeling, we considered no spatial temperature variation in the fuel cell. All the components of the cell like electrode, inter connector, and gas inside the channels are at the same temperature. It is further assumed that the heat capacity of the gases inside the channels are negligible compared to the solid components of the fuel cell. Then the dynamic model of the cell temperature can be found by performing energy balance around the entire fuel cell stack. If  $H_i$  is the molar enthalpy of  $i^{th}$  species in the fuel and air streams, the energy balance is as below.

$$m_s C_{ps} \frac{dT_s}{dt} = \sum \dot{n}_i^{in} H_i^{in} - \sum \dot{n}_i^{out} H_i^{out} - \dot{n}_{H_2}^r \Delta \hat{H}_r^0 - V_s I$$

where  $T_s$  is the stack temperature,  $m_s$  is mass of stack and  $C_{ps}$  is average specific heat of fuel cell materials excluding gases,  $\Delta \hat{H}_r^0$  is the heat of reaction (calculated using NASA polynomials [20]),  $V_s$  is stack voltage and  $I$  is current.

### Schematic Simulink Model of Non-isothermal SOFC

The above discussed lumped model of non-isothermal SOFC with unchoked flow is modeled in MATLAB Simulink as



### 3.2.2 Results

After simulations of the above lumped model of non-isothermal SOFC in MATLAB Simulink, we observe that V-I curve from the simulation follows same trend as theoretical V-I curve given by [1].

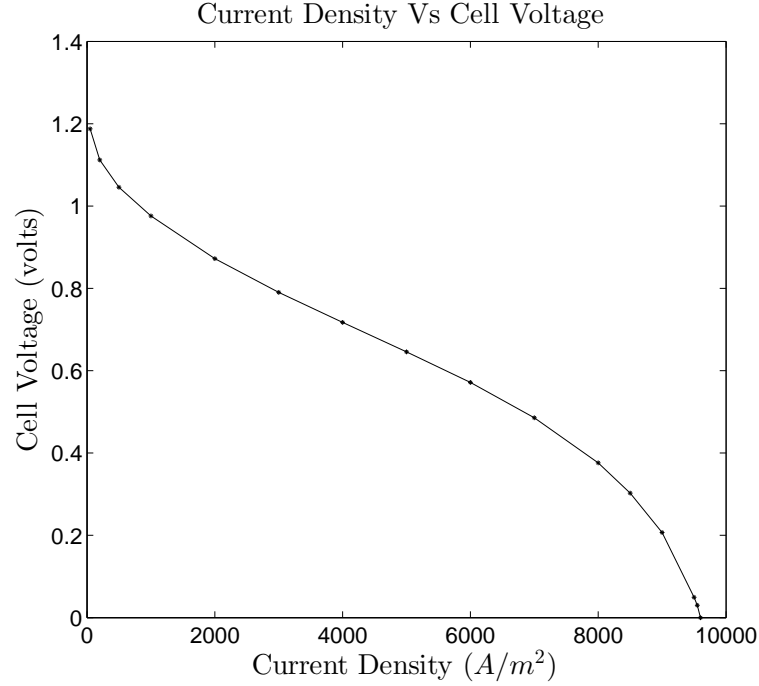


Figure 3.7: Voltage of nonisothermal SOFC at fuel flow rate is 2 mole/sec, air flow rate is 5 mole/sec

For a step up in fuel flow rate from 2 to 2.5 mole/sec and step up in current from 400 to 500A then dynamics of voltage and temperature curves are as expected. Dynamics of ohmic, activation and concentration polarization curves are presented below. Figure 3.6 shows the steady state voltage output from the lumped model at various currents which is the V-I curve. It can be seen that voltage decreases with current density in the simulated range. Figure 3.7 illustrates the dynamics of voltage for non-isothermal SOFC. Initially voltage increases because pressure inside cell increases and then voltage decreases due to increase in temperature which finally reaches steady state. Figure 3.8 shows the dynamics of temperature for non-isothermal SOFC. temperature increases because of heat of the reaction. Figure 3.9 will be used to illustrate dynamics of voltage when step up fuel flow rate from 2 to 2.5 mole/sec. Steady state voltage increase because increase in reactant pressures inside the fuel cell and also observed that dynamics are slow because of dynamics of temperature. Figure 3.10 shows the temperature dynamics when step up fuel flow rate from 2 to 2.5 mole/sec. Temperature decreases because of extra reactants flow cools the fuel cell. Figure 3.11 shows the dynamics of voltage when step up in current from 400 to 500A. Voltage decreases because of increase in activation polarization and ohmic polarization. Figure 3.12 shows the dynamics of temperature for a step in current from 400 to 500A. Temperature increase due to heat of reaction. Figure 3.13 shows the dynamics of activation polarization. Voltage loss increases due to increase in temperature of cell. Figure 3.14 shows the dynamics of ohmic polarization. Voltage loss decreases due to increase in temperature that decrease resistance offered by electrolyte. Figure 3.15 illustrates the dynamics of concentration loss. Voltage loss increase due to increase in temperature.

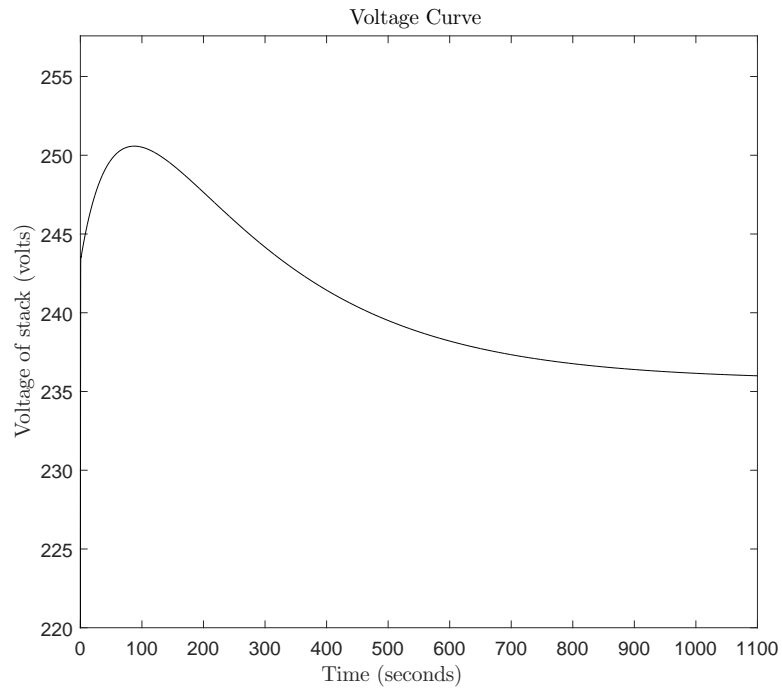


Figure 3.8: Voltage of non-isothermal SOFC at fuel flow rate is  $2 \text{ mole/sec}$ , air flow rate is  $5 \text{ mole/sec}$  and current is  $400A$

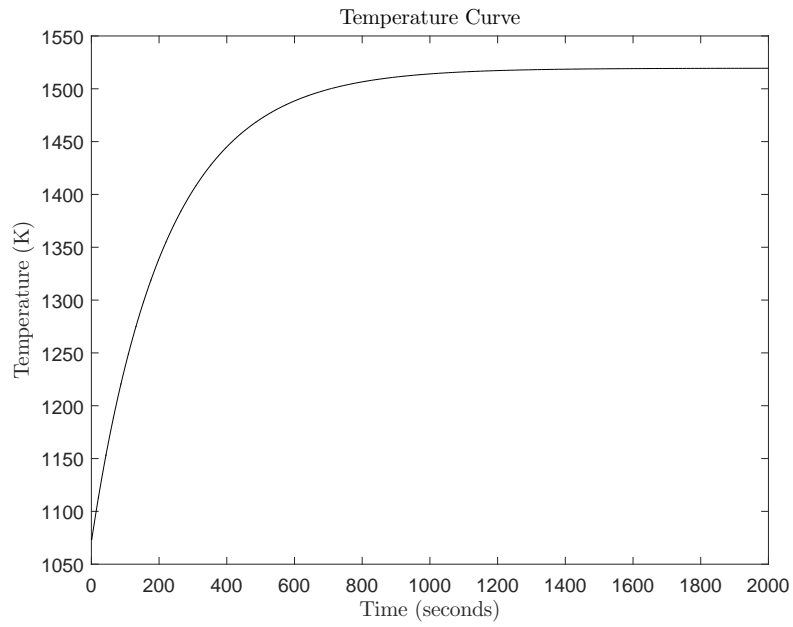


Figure 3.9: Temperature of non-isothermal SOFC at fuel flow rate is  $2 \text{ mole/sec}$ , air flow rate is  $5 \text{ mole/sec}$  and current is  $400A$

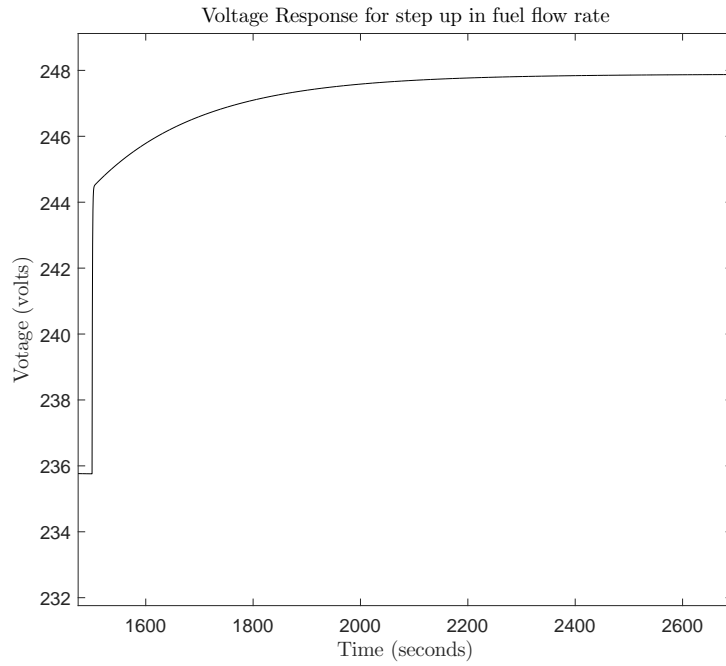


Figure 3.10: Voltage curve for step up in fuel flow rate from 2 to 2.5 *mole/sec* at air flow rate is 5 *mole/sec* and current is 400A

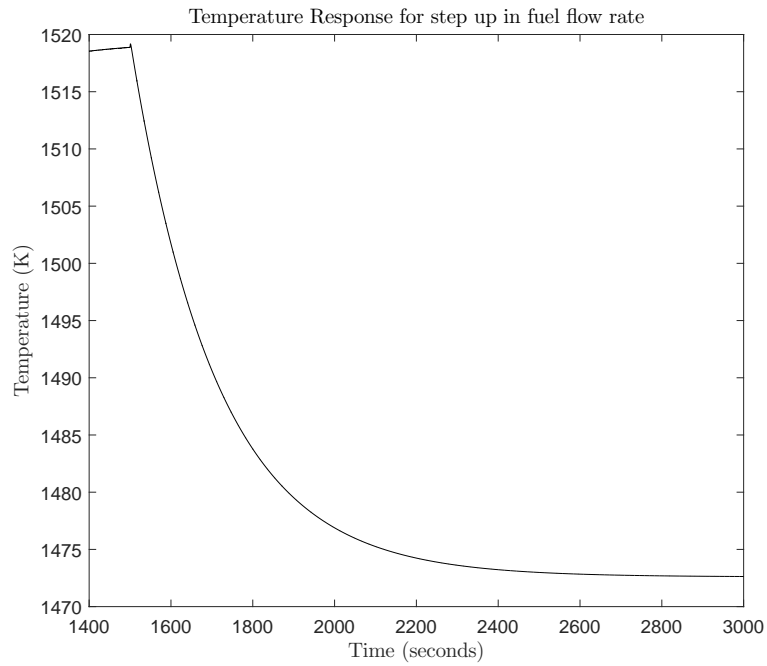


Figure 3.11: Temperature curve for step up in fuel flow rate from 2 to 2.5 *mole/sec* at air flow rate is 5 *mole/sec* and current is 400A

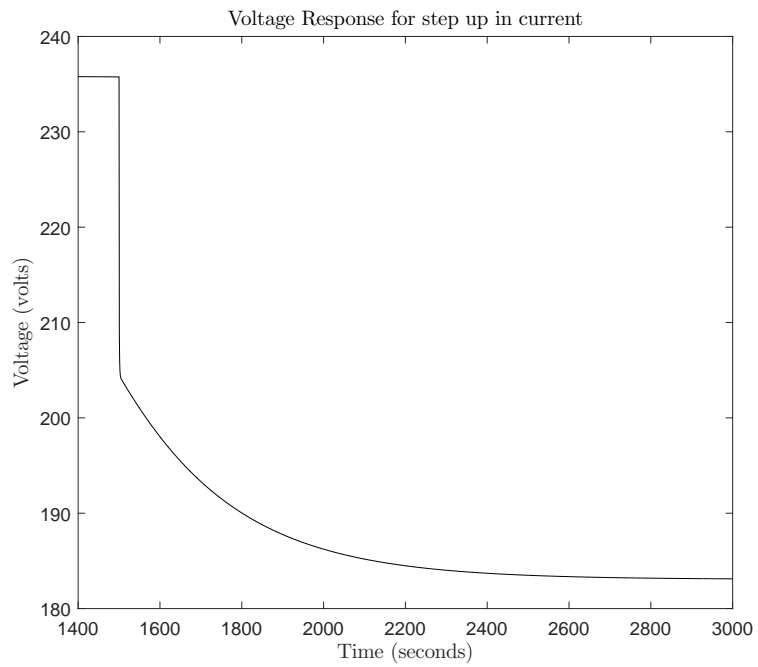


Figure 3.12: Voltage curve for step up in current from 400 to 500A, at fuel flow rate is 2 mole/sec, air flow rate is 5 mole/sec

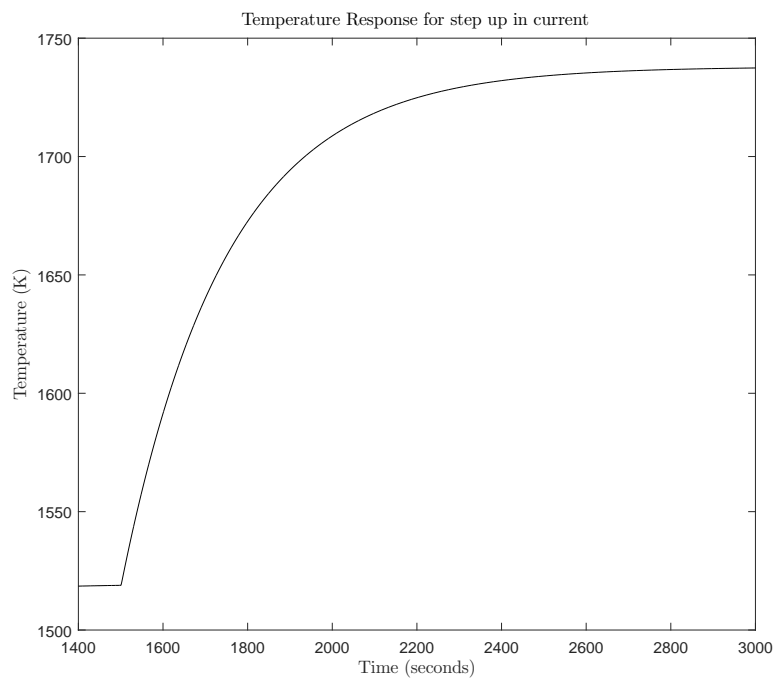


Figure 3.13: Temperature curve for step up in current from 400 to 500A, at fuel flow rate is 2 mole/sec, air flow rate is 5 mole/sec

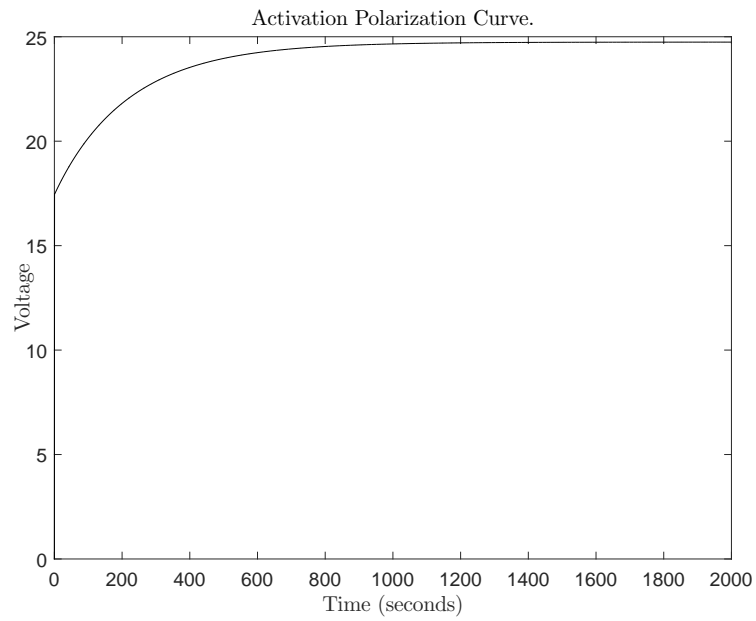


Figure 3.14: Activation polarization curve at fuel flow rate is  $2 \text{ mole/sec}$ , air flow rate is  $5 \text{ mole/sec}$  and current is  $400A$

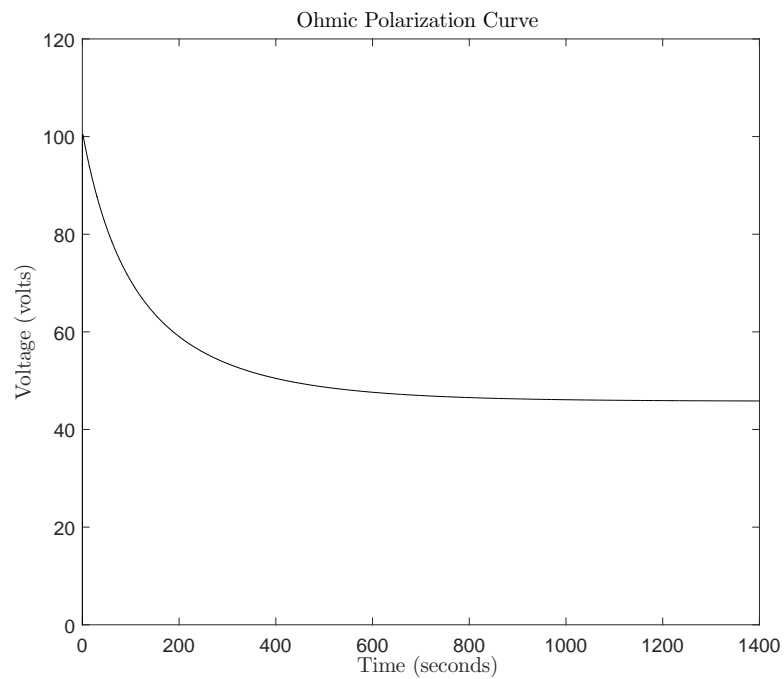


Figure 3.15: Ohmic polarization curve at fuel flow rate is  $2 \text{ mole/sec}$ , air flow rate is  $5 \text{ mole/sec}$  and current is  $400A$

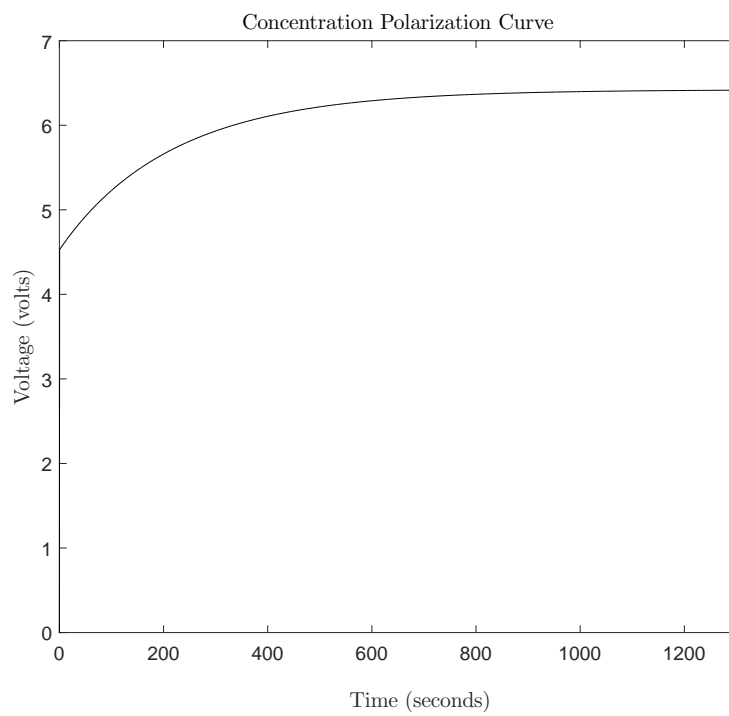


Figure 3.16: Concentration polarization curve at fuel flow rate is  $2 \text{ mole/sec}$ , air flow rate is  $5 \text{ mole/sec}$  and current is  $400A$



## Chapter 4

# Linear Controller And Gain Scheduling Design

The main requirements of the controller are to give faster response in disturbance rejection and set point tracking. There are three main methods for designing nonlinear controllers

**Controller design based on gain scheduling** To compute a linear model for the nonlinear plant, the most common approach is based on Jacobian linearization of the nonlinear model about an operating point (equilibrium point). Dynamics of linear and nonlinear models are will be similar close to the operating point, so we can design a controller for the linear model, and use this controller for the nonlinear plant at that operating point. If we operate nonlinear plant away from operating point, these linear controllers do not give good performance.

When the nonlinear process needs to be controlled in a wide range of process parameters, gain scheduling is used. Gain scheduling is based on designing linear controllers at multiple operating points and switching between them based on process variables.

**Controller design based on feedback linearization** In this method, we obtain a new transformation that can convert a nonlinear differential equation to linear differential equation. It is systematic and more accurate but it depends upon complicated design procedures and is not suitable to handle constraints in a systematic manner. One of the such systematic nonlinear control methods is full state feedback linearization.

**Optimal controller** Optimal control deals with the problem of finding a control law for a given system such that a certain optimality criterion is achieved. A control problem includes a cost functional that is a function of state and control variables. An optimal control is a set of differential equations describing the paths of the control variables that minimize the cost functional. It can handle the constrains on control variable. Model Predictive Control is an approximation approach to optimal control [21].

## 4.1 Control Design by Approximate Linearization

Consider the nonlinear system

$$\dot{x} = f(x, u); \quad f : x \in \mathcal{R}^n; u \in \mathcal{R}^m \quad (4.1)$$

$$y = g(x, u); \quad g : x \in \mathcal{R}^n; u \in \mathcal{R}^m \quad (4.2)$$

where  $f, g, x, u$  are vectors defined as  $f = [f_1 \ f_2 \ f_3 \ \dots \ f_n]$ ,  $g = [g_1 \ g_2 \ g_3 \ \dots \ g_n]$ ,  $x = [x_1 \ x_2 \ x_3 \ \dots \ x_n]$  and  $u = [u_1 \ u_2 \ u_3 \ \dots \ u_m]$ .

The objective is to control this system at the operating point  $(x_0, u_0)$ . For suppose that  $(x_0, u_0)$  is a point such that  $f(x, u) = 0$ . In this case, the point  $(x_0, u_0)$  is called an equilibrium point of the system  $\dot{x} = f(x, u)$ . Here  $f(x, u)$  is a nonlinear function with multiple variables. Using Taylor series expansion we can express nonlinear function  $f(x, u)$  around the point  $(x_0, u_0)$  is given by

$$f(x, u) = f(x_0, u_0) + \left. \frac{\partial f}{\partial x} \right|_{(x_0, u_0)} (x - x_0) + \left. \frac{\partial f}{\partial u} \right|_{(x_0, u_0)} (u - u_0) + O(x - x_0)^2 + O(u - u_0)^2$$

For  $(x, u)$  sufficiently close to  $(x_0, u_0)$ , then higher order terms  $(O(x - x_0)^2 + O(u - u_0)^2)$  will be very close to zero, so we can neglect them to obtain the approximation

$$f(x, u) \approx f(x_0, u_0) + \left. \frac{\partial f}{\partial x} \right|_{(x_0, u_0)} (x - x_0) + \left. \frac{\partial f}{\partial u} \right|_{(x_0, u_0)} (u - u_0)$$

since  $f(x_0, u_0) = 0$ , approximate nonlinear state equation as

$$\dot{x} = \left. \frac{\partial f}{\partial x} \right|_{(x_0, u_0)} (x - x_0) + \left. \frac{\partial f}{\partial u} \right|_{(x_0, u_0)} (u - u_0)$$

We define  $\Delta x = x - x_0$  and  $\Delta u = u - u_0$ . Here  $\Delta x$ ,  $\Delta u$  are deviation variables and  $\dot{x} = \Delta \dot{x}$ . Now we can write nonlinear state equation in terms of deviation variables as

$$\Delta \dot{x} = \left. \frac{\partial f}{\partial x} \right|_{(x_0, u_0)} (\Delta x) + \left. \frac{\partial f}{\partial u} \right|_{(x_0, u_0)} (\Delta u)$$

where matrices  $A = \left. \frac{\partial f}{\partial x} \right|_{(x_0, u_0)}$ ,  $B = \left. \frac{\partial f}{\partial u} \right|_{(x_0, u_0)}$  are Jacobean matrices as

$$A = \begin{bmatrix} \frac{\partial f_1}{\partial x_1} & \frac{\partial f_1}{\partial x_2} & \frac{\partial f_1}{\partial x_3} & \cdot & \cdot & \cdot & \frac{\partial f_1}{\partial x_n} \\ \frac{\partial f_2}{\partial x_1} & \frac{\partial f_2}{\partial x_2} & \frac{\partial f_2}{\partial x_3} & \cdot & \cdot & \cdot & \frac{\partial f_2}{\partial x_n} \\ \cdot & \cdot & \cdot & \cdot & \cdot & \cdot & \cdot \\ \cdot & \cdot & \cdot & \cdot & \cdot & \cdot & \cdot \\ \frac{\partial f_n}{\partial x_1} & \frac{\partial f_n}{\partial x_2} & \frac{\partial f_n}{\partial x_3} & \cdot & \cdot & \cdot & \frac{\partial f_n}{\partial x_n} \end{bmatrix}$$

To be continue

$$B = \begin{bmatrix} \frac{\partial f_1}{\partial u_1} & \frac{\partial f_1}{\partial u_2} & \frac{\partial f_1}{\partial u_3} & \cdot & \cdot & \frac{\partial f_1}{\partial u_m} \\ \frac{\partial f_2}{\partial u_1} & \frac{\partial f_2}{\partial u_2} & \frac{\partial f_2}{\partial u_3} & \cdot & \cdot & \frac{\partial f_2}{\partial u_m} \\ \cdot & \cdot & \cdot & \cdot & \cdot & \cdot \\ \cdot & \cdot & \cdot & \cdot & \cdot & \cdot \\ \frac{\partial f_n}{\partial u_1} & \frac{\partial f_n}{\partial u_2} & \frac{\partial f_n}{\partial u_3} & \cdot & \cdot & \frac{\partial f_n}{\partial u_m} \end{bmatrix}$$

Final deviation variable of linear state equation for nonlinear state equation is

$$\Delta \dot{x} = A(\Delta x) + B(\Delta u) \quad (4.3)$$

For nonlinear output equation(4.2), we follow the same procedure to get approximate linear output equation around  $(x_0, u_0)$  and observe similar expression for  $y = g(x, u)$  as

$$y = g(x_0, u_0) + \frac{\partial g}{\partial x} \Big|_{(x_0, u_0)} (x - x_0) + \frac{\partial g}{\partial u} \Big|_{(x_0, u_0)} (u - u_0)$$

where  $y_0 = g(x_0, u_0)$  is output we get at operating point. define  $\Delta y = y - y_0$ . we can write the linear output equation as

$$\Delta y = \frac{\partial g}{\partial x} \Big|_{(x_0, u_0)} \Delta x + \frac{\partial g}{\partial u} \Big|_{(x_0, u_0)} \Delta u$$

where matrices  $C = \frac{\partial g}{\partial x} \Big|_{(x_0, u_0)}$ ,  $D = \frac{\partial g}{\partial u} \Big|_{(x_0, u_0)}$  are Jacobean matrices as

$$C = \begin{bmatrix} \frac{\partial g_1}{\partial x_1} & \frac{\partial g_1}{\partial x_2} & \frac{\partial g_1}{\partial x_3} & \cdot & \cdot & \frac{\partial g_1}{\partial x_n} \\ \frac{\partial g_2}{\partial x_1} & \frac{\partial g_2}{\partial x_2} & \frac{\partial g_2}{\partial x_3} & \cdot & \cdot & \frac{\partial g_2}{\partial x_n} \\ \cdot & \cdot & \cdot & \cdot & \cdot & \cdot \\ \cdot & \cdot & \cdot & \cdot & \cdot & \cdot \\ \frac{\partial g_p}{\partial x_1} & \frac{\partial g_p}{\partial x_2} & \frac{\partial g_p}{\partial x_3} & \cdot & \cdot & \frac{\partial g_p}{\partial x_n} \end{bmatrix}$$

$$D = \begin{bmatrix} \frac{\partial g_1}{\partial u_1} & \frac{\partial g_1}{\partial u_2} & \frac{\partial g_1}{\partial u_3} & \cdot & \cdot & \frac{\partial g_1}{\partial u_m} \\ \frac{\partial g_2}{\partial u_1} & \frac{\partial g_2}{\partial u_2} & \frac{\partial g_2}{\partial u_3} & \cdot & \cdot & \frac{\partial g_2}{\partial u_m} \\ \cdot & \cdot & \cdot & \cdot & \cdot & \cdot \\ \cdot & \cdot & \cdot & \cdot & \cdot & \cdot \\ \frac{\partial g_p}{\partial u_1} & \frac{\partial g_p}{\partial u_2} & \frac{\partial g_p}{\partial u_3} & \cdot & \cdot & \frac{\partial g_p}{\partial u_m} \end{bmatrix}$$

Final deviation output of linear state equation for nonlinear output is

$$\Delta y = C(\Delta x) + D(\Delta u) \quad (4.4)$$

Design a feedback control for linear state space model (4.3), (4.4), obtained above by approximate linearization of nonlinear model around  $(x_0, u_0)$ . Block diagram as shown in figure (4.1)

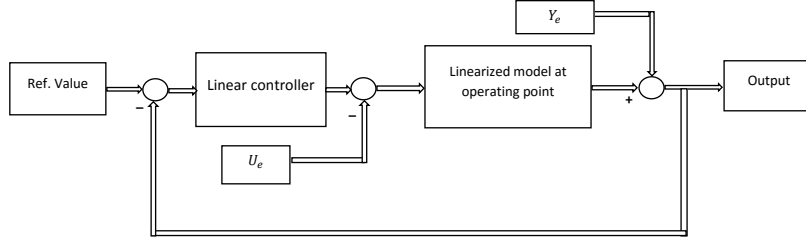


Figure 4.1: Linear feedback control design

Apply the feedback linear control design for linear state space model to nonlinear plant around operating point  $(x_0, u_0)$ . Block diagram as shown in figure (4.2).

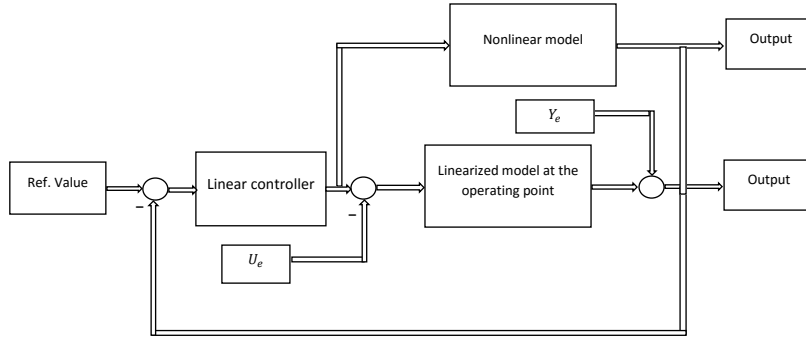


Figure 4.2: Implementation of linear control for nonlinear plant

#### 4.1.1 Approximate Linear Control Design For SOFC

We have done dynamic modeling of isothermal SOFC in chapter (3) and observed that state, output equations contains highly nonlinear functions. The operating point for isothermal SOFC system is  $x_{op} = [4.55e4 \ 5.63e4 \ 1.35e4 \ 9.66e4]$  at fuel flow rate and current extract from fuel cell,  $u_0 = [2400]$  and output is  $y_0 = 240$ . Linearization of nonlinear isothermal mmodel at operating point  $(x_{op}, u_0)$  using above mentioned procedure. we obtain

$$\Delta \dot{x} = A(\Delta x) + B(\Delta u)$$

$$\Delta y = C(\Delta x) + D(\Delta u)$$

where  $x = [P_{H_2} \ P_{H_2O} \ P_{O_2} \ P_{N_2}]$ ,  $u = [u_f \ I]$ ,  $y = V$  (voltage) and

$$A = \begin{bmatrix} -44.09 & -44.64 & 0 & 0 \\ -44.61 & -45.23 & 0 & 0 \\ 0 & 0 & -3.713 & -1.536 \\ 0 & 0 & -11.1 & -13.14 \end{bmatrix}$$

$$B = \begin{bmatrix} -105.1 & 52820 \\ 105.1 & 0 \\ -52.56 & 0 \\ 0 & 0 \end{bmatrix}$$

$$C = \begin{bmatrix} 0.0004112 & -0.0004154 & 0.007797 & 0 \end{bmatrix}$$

$$D = \begin{bmatrix} -0.1734 & 0 \end{bmatrix}$$

We design feedback linear control (PID) for above obtained linear state space model for isothermal SOFC. Gains are calculate using auto tuning PID in matlab simulink as shown in figure (4.3)

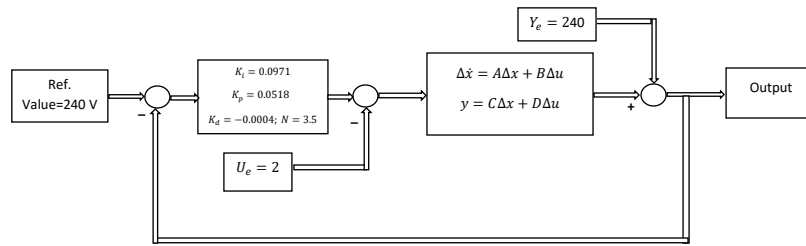


Figure 4.3: Feedback linear control design

Gains obtained by auto tuning PID are  $[K_p \ K_i \ K_d \ N] = [0.0571 \ 0.0971 \ -0.0004 \ 3.5]$ . Apply design feedback linear control (PID) to nonlinear isothermal SOFC as shown in figure (4.4)

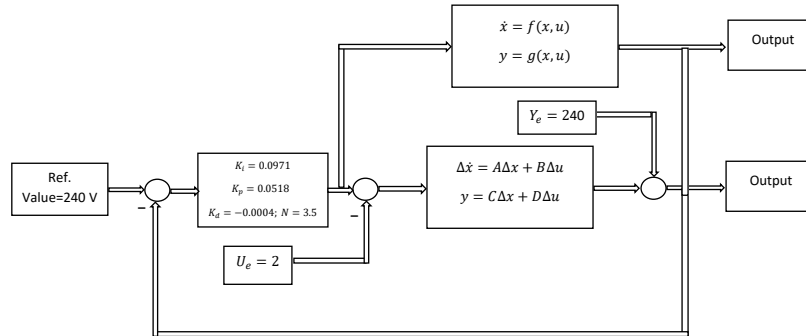


Figure 4.4: Implement linear control to nonlinear SOFC

## 4.1.2 Result

After implementation of a linear control to isothermal SOFC we observe that linear control gives very good performance around the operating point  $(x_0, u_0)$ . If we apply this control away from the operating point then linear control does not give efficient results.

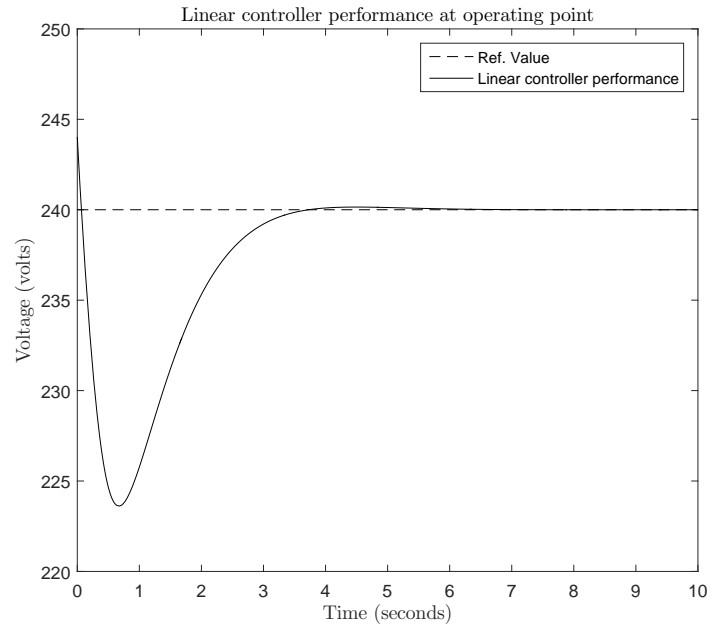


Figure 4.5: Linear control action at operating point

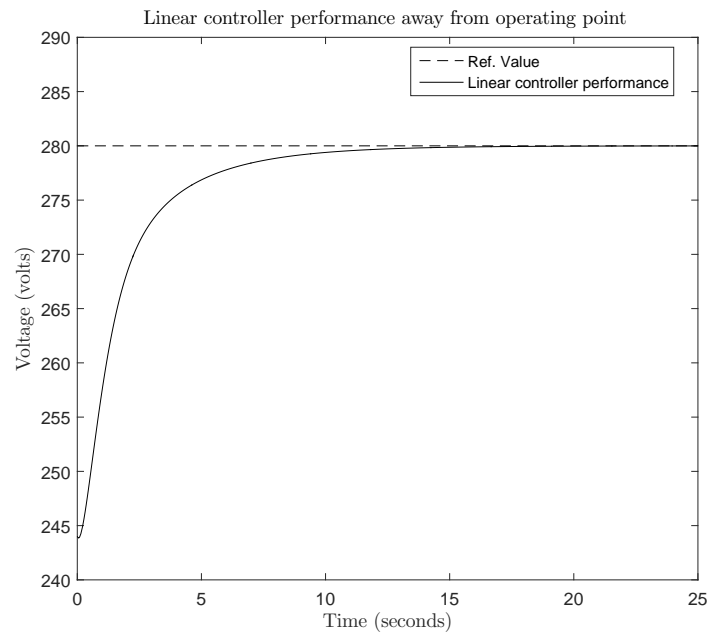


Figure 4.6: Linear control action away from operating point

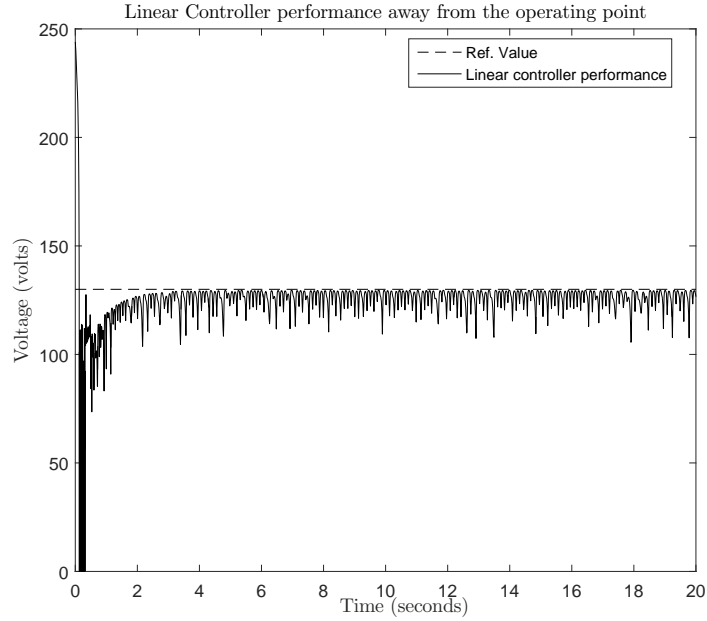


Figure 4.7: Linear control action away from operating point

Figure 4.5 shows the performance of linear control at operating point and desire output is 240V. With in 5 seconds it reaches desirable output. Figure 4.6 shows the performance of the linear control away from the operating point. The desirable output change from 240 to 280V. Control action given by linear control is slow because of the gains required for new operating point are less than gains used in applied linear control. Figure 4.7 shows the performance of the linear control away from the operating point. The desirable output change from 240 to 130V. Control action given by linear control is fast and getting fluctuation in output because of the gains required for new operating point are greater than gains used in applied linear control. Above mentioned issues can be solved using gain scheduling controller.

## 4.2 Control Design Using Gain Scheduling

Gain scheduling is an approach to control of non-linear systems that uses a family of linear controllers. Each of them provides a satisfactory control for a different operating points of the nonlinear isothermal SOFC given in chapter (3). Each of which provides satisfactory control for different operating points of the system. A gain-scheduled controller is a controller whose gains are automatically adjusted as a function of time, output and operating condition or plant parameters.

### Procedure for Design Gain Scheduling Controller

1. Select a set of operating points that adequately covers the operating range of variables on which the gain depends.
2. Build a collection of linear models describing the linearized plant dynamics at selected design points. The tabulated gains for each operating point for the SOFC system are :

Gains With process variable(output)				
Voltage	$K_p$	$K_i$	$K_d$	N
140	0.0003806	0.000388	-0.00037	1.809
160	0.0011	0.00116	-0.0001	1.8207
200	0.006592	0.00758	-0.00038	1.735
230	0.03763	0.04756	-0.0004	3.35
240	0.0518	0.0971	-0.00041	3.569
245	0.0743	0.124	-0.0004	4.419
250.8	0.08468	0.2033	-0.000045	4.587
260	0.129	0.403	-0.00055	5.94

3. Formulate gains as a function of process variable (voltage), based on gains vs process variable data. In Matlab Simulink, we can use lookup tables.

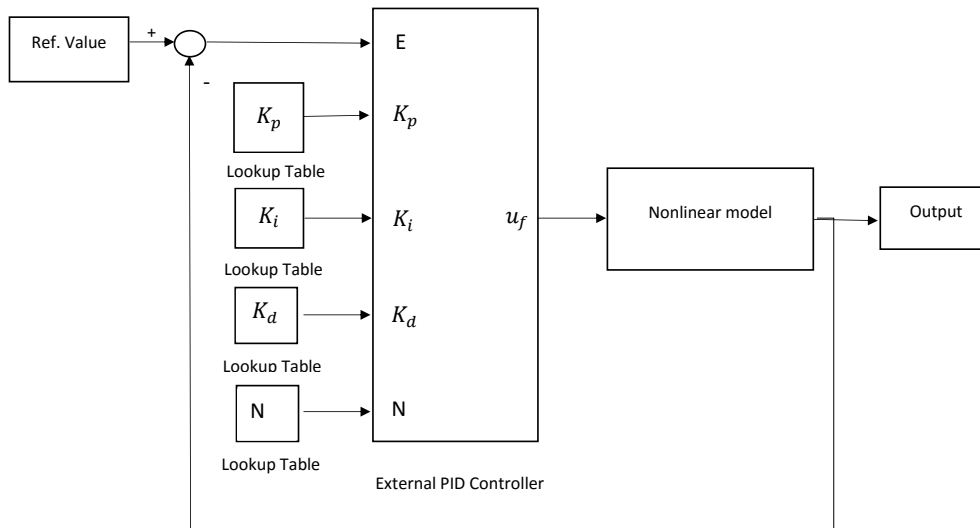


Figure 4.8: Schematic block diagram for implementation of gain scheduling controller

4. Implement gain scheduling controller to a nonlinear plant. For SOFC, a comparison of linear control and gain scheduling control is presented in next sections.

#### 4.2.1 Results

Gain scheduling control gives very good performance over the operating range. We compared the results with that of a linear controller described in the previous sections.



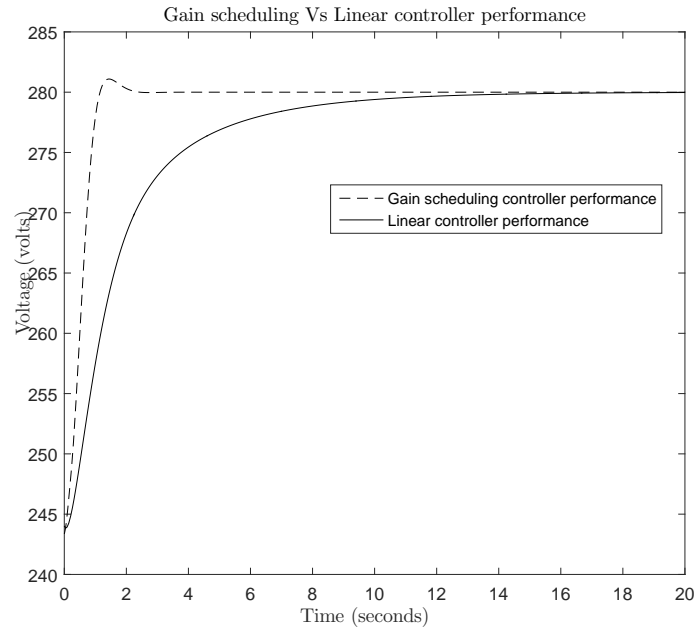


Figure 4.9: Comparison of response of linear controller and gain scheduling controller

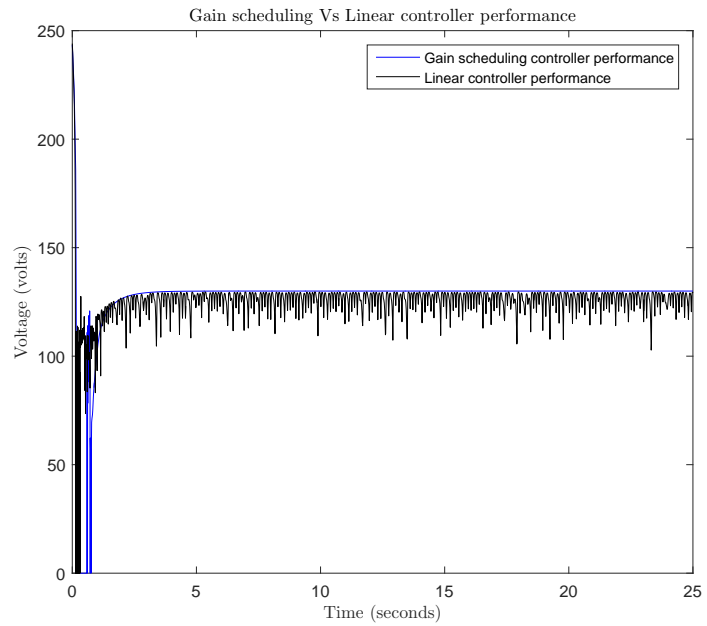


Figure 4.10: Comparison of response of linear controller and gain scheduling controller

It can be observed clearly that gain scheduling control resolved the earlier mentioned problems

## Chapter 5

# Nonlinear Controllability And Observability

### 5.1 Controllability

Controllability is an important property of a control system, and the controllability property plays a crucial role in many control problems, such as stabilization of unstable systems by feedback. Consider the  $n$ -dimensional and  $p$ -input state equation

$$\dot{x} = Ax + Bu \quad (5.1)$$

Where  $A$  and  $B$  are constant matrices having dimensions of  $n \times n$  and  $n \times p$  respectively. The control variable  $u$  represents the externally applied controls. The state variable  $x$  may or may not be directly measurable and is used to represent then memory of the system. The past history of system affects its future evolution.

**Definition of Controllability** The state equation (5.1) is said to be controllable if for any initial state  $x_0$  and any final state  $x_1$ , there exists an input that transfers  $x_0$  to  $x_1$  in a finite time. Otherwise equation (5.1) is said to be uncontrollable.

**Controllability For Linear Systems** For Linear systems, it has been shown that [14] the controllability condition reduces to the matrix  $C = [B \ AB \ A^2B \ \dots \ A^{n-1}B]$  being full row rank.

#### 5.1.1 Controllability For Nonlinear System

Consider a nonlinear System given by

$$\frac{dx}{dt} = f(x) + \sum g_i(x)u; \quad i = 1, 2, \dots, m \quad (5.2)$$

$$y = h(x) \quad (5.3)$$

we can check the controllability at an operating point, using linearization to get equivalent linear system. The Controllability rank condition is not valid away from the operating point. By using differential geometry we can obtain controllability condition which is globally valid.

### 5.1.2 Controllability of Nonlinear Systems Using Differential Geometry

Consider the nonlinear system introduced above. Note that here  $f, g_i; i = 1, 2, 3, \dots, m$  are vector fields. We first define the concept of a Lie bracket.

**Lie Bracket** For two vector fields  $f$  and  $g$  on some domain  $D \in R^n$ , the Lie bracket  $[f, g]$  is a third vector field denoted by

$$[f, g] = \left\langle \frac{\partial g}{\partial x}, f \right\rangle - \left\langle \frac{\partial f}{\partial x}, g \right\rangle$$

where  $\frac{\partial g}{\partial x}$  and  $\frac{\partial f}{\partial x}$  are Jacobian matrices [4]. We may repeat bracketing of  $g$  with  $f$ . The following notation is

$$\begin{aligned} ad_f^0 g(x) &= g(x) \\ ad_f^1 g(x) &= [f, g](x) \\ ad_f^2 g(x) &= [f, ad_f^1 g](x) \\ ad_f^k g(x) &= [f, ad_f^{k-1} g](x), \quad k \geq 1 \end{aligned}$$

For single input case, the controllability condition is that  $C = [ad_f^0 g(x) \quad ad_f^1 g(x) \quad ad_f^2 g(x) \dots ad_f^k g(x)]$  has full row rank, otherwise system is not controllable. In the multiple input case, let  $C_i$  be the controllability matrix for the  $i^{th}$  input. The controllability condition is that  $C = [C_1, C_2, \dots]$  has full row rank.

### 5.1.3 Controllability of Isothermal SOFC Using Differential Geometry

The Isothermal SOFC state equations after substituting constant parameter are

$$\frac{dx}{dt} = f(x) + \Sigma g_i(x)u; \quad i = 1, 2, 3 \quad (5.4)$$

$$f_1(x) = -99.24P_{H_2} \sqrt{\frac{2(P_{H_2} + P_{H_2O} - 101325)}{10.58P_{H_2} + 95.26P_{H_2O}}}$$

$$f_2(x) = -99.24P_{H_2O} \sqrt{\frac{2(P_{H_2} + P_{H_2O} - 101325)}{10.58P_{H_2} + 95.26P_{H_2O}}}$$

$$f_3(x) = -99.24P_{O_2} \sqrt{\frac{2(P_{O_2} + P_{N_2O} - 101325)}{148.19P_{O_2} + 169.36P_{N_2}}}$$

$$f_4(x) = -99.24P_{N_2} \sqrt{\frac{2(P_{O_2} + P_{N_2O} - 101325)}{148.19P_{O_2} + 169.36P_{N_2}}}$$

where  $x, f$  are defined as  $x = [P_{H_2} \quad P_{H_2O} \quad P_{O_2} \quad P_{N_2}]'$ ,  $f(x) = [f_1(x) \quad f_2(x) \quad f_3(x) \quad f_4(x)]'$

This system has three inputs,

- 1 Fuel flow rate corresponding  $g$  vector field is  $g_1 = [5.29e04 \ 0 \ 0 \ 0]'$
- 2 Air flow rate corresponding  $g$  vector field is  $g_2 = [0 \ 0 \ 1.11e04 \ 4.181e04]'$
- 3 Current extracted from fuel cell corresponding  $g$  vector field is  $g_3 = [-105.84 \ 105.84 \ -52.65 \ 0]'$

We first calculate matrix  $C_1$  (for fuel flow rate input) using above mentioned procedure, here vector fields are  $f, g_1$  and then calculate matrix  $C_2$  (for air flow rate input) using  $f, g_2$  vector fields and finally calculate matrix  $C_3$  (for current input) using  $f, g_3$  vector fields. The over-all matrix  $C = [C_1, C_2, C_3]$  has been observed to have full row rank (i.e. equal to four). It has been checked that for all  $x$ , the rank of the matrix  $C$  is equal to four. Hence, the isothermal SOFC is controllable globally.

## 5.2 Observability

Observability is an important property of a control system, and the Observability property plays a crucial role in estimation of states for example using Kalman or Particle Filters..

**Definition of Observability** Consider system described by (5.3) and (5.4). Two states  $x_0, x_1$  are said to be distinguishable if there exists an input function  $u(\cdot)$  such that

$$y(\cdot, x_0, u) \neq y(\cdot, x_1, u)$$

where  $y(\cdot, x_0, u)$ ,  $i = 1, 2$  is the output function of the system (5.3),(5.4) corresponding to input function  $u(\cdot)$  and the initial condition  $x(0) = x_i$ . The system said to be locally observable at  $x_0 \in X$  if there exists a neighborhood  $N$  of  $x_0$  such that every  $x \in N$  other than  $x_0$  is distinguishable from  $x_0$ . The system is said to be observable if it is locally observable at each  $x_0 \in X$  [4].

**Observability For Linear Systems** Consider the linear system given by

$$\frac{dx}{dt} = Ax + Bu; \tag{5.5}$$

$$y = Cx + Du \tag{5.6}$$

This system is called observable if the rank of  $O = [C \ CA \ CA^2 \ \dots \ CA^{n-1}]'$  is  $n$  [14].

### 5.2.1 Observability For Nonlinear Systems

Consider the nonlinear system given by equation (5.2), (5.3). we can check the controllability at an operating point, using linearization to get equivalent linear system. However, such guarantees are not valid away from the operating point. By using differential geometry we can obtain observability condition which is globally valid [4].

### 5.2.2 Observability For Nonlinear System Using Differential Geometry

Consider the nonlinear system introduced above by equations (5.2), (5.3). Note that here  $f, g_i; i = 1, 2, 3, \dots, m$  are vector fields and  $h$  is smooth function.

**Theorem 1** *It is sufficient condition for local observability. Consider the system described by (5.2) and (5.3), and suppose  $x_0 \in X$  is given. Consider the form*

$$(dL_{z_s}L_{z_{s-1}}\dots\dots L_{z_1}h_j)(x_0), s \geq 0, z_i \in \{f, g_1, \dots, g_m\} \quad (5.7)$$

*evaluated at  $x_0$ . Suppose there are  $n$  linearly independent row vectors in this set. Then the system is locally observable around  $x_0$ .*

where  $L_f h$  Lie derivative of the function  $h(x)$  with respect to vector field  $f$  defined by  $L_f h = \langle dh, f \rangle$ , where  $dh$  is a differential form defined as row vector  $[\frac{\partial h}{\partial x_1} \dots \dots \frac{\partial h}{\partial x_n}]$ . To find observability condition we follow a procedure similar to the linear case. First generate  $O$  matrix with row vectors from all combinations of (5.7) and then calculate rank of matrix  $O$ . If the rank is  $n$  then system is locally observable at  $x_0$ . The system is said to be observable it is locally observable at each  $x_0 \in X$  [4].

### 5.2.3 Observability For Isothermal SOFC Using Differential Geometry

Consider the isothermal SOFC state equation described above in section (5.1.3). In this model vector fields are  $f, g_1, g_2, g_3$  and output voltage given in section (3.1.7). The output is a smooth function  $h(x) = V$ . The matrix  $O$  is obtained from combinations of  $dh, dL_f h, dL_{g_1} h, dL_{g_2} h, dL_{g_3} h, dL^2_f h, dL_f L_{g_1} h, dL_f L_{g_2} h, dL_f L_{g_3} h \dots$  and so on. For all  $x$  the rank matrix  $O$  is four and hence SOFC is observable globally. Therefore, we can estimate states of our isothermal SOFC system using input-output data.

## Chapter 6

# Feedback Linearization Controller Design

Feedback linearization is also known as exact linearization. In approximate linearization we truncate higher order terms in Taylor expansion thereby losing information while in exact linearization we transform the nonlinear system into an equivalent linear system. There are two types of feedback linearization, one is full state feedback linearization and other one is input-output linearization. SOFC system have state and output equation which are nonlinear. In this chapter we discuss full state feedback linearization assuming that the states are measured.

### 6.1 Full-State Feedback Linearization

We consider nonlinear system given by

$$\dot{x} = f(x) + g(x)u \quad (6.1)$$

The idea in state feedback linearization is to transform the above non-linear equation and design control variable such that we can get an equivalent linear equation with  $v$  as input and  $z$  as states.

$$\dot{z} = A_c z + B_c v \quad (6.2)$$

We first transform the nonlinear state equation (6.1) by  $z = T(x)$  ( $T$  should be a diffeomorphism) to get

$$\dot{z} = A_c z + B_c \gamma(x)[u - \alpha(x)] \quad (6.3)$$

where we identify  $u = \alpha(x) + \beta(x)v$  and  $\gamma(x) = 1/\beta(x)$ . The main questions now are 1) whether there exist a such  $u, T$  and 2) how to estimate  $\alpha(x)$ ,  $\beta(x)$  and  $T$ . There exists a systematic procedure [5] to calculate  $T, \alpha(x)$  and  $\beta(x)$ .

**Procedure:** First we write dynamic model state equation in terms of  $z$

$$\dot{z} = \frac{\partial T}{\partial x} \dot{x}$$

substituting  $\dot{x}$  expression given in equation (6.1)

$$\dot{z} = \frac{\partial T}{\partial x} [f(x) + g(x)u] \quad (6.4)$$

Comparing with the desired equation,

$$\begin{aligned} A_c z + B_c \gamma(x)[u - \alpha(x)] &= \frac{\partial T}{\partial x} [f(x) + g(x)u] \\ \frac{\partial T}{\partial x} f(x) &= A_c z - B_c \gamma(x)\alpha(x) \\ \frac{\partial T}{\partial x} g(x) &= B_c \gamma(x) \end{aligned} \quad (6.5)$$

These are equivalent to

$$\begin{aligned} \frac{\partial T_1}{\partial x} f(x) &= T_2(x) \\ \frac{\partial T_2}{\partial x} f(x) &= T_3(x) \\ &\vdots \\ \frac{\partial T_{n-1}}{\partial x} f(x) &= T_n(x) \\ \frac{\partial T_n}{\partial x} f(x) &= -\gamma(x)\alpha(x) \end{aligned}$$

and

$$\begin{aligned} \frac{\partial T_1}{\partial x} g(x) &= 0 \\ \frac{\partial T_2}{\partial x} g(x) &= 0 \\ &\vdots \\ \frac{\partial T_{n-1}}{\partial x} g(x) &= 0 \\ \frac{\partial T_n}{\partial x} g(x) &= \gamma(x) \end{aligned}$$

where  $T = [T_1; T_2; T_3; \dots; T_n]$ . If we take  $T_1(x) = h(x)$  we obtain

$$T_{i+1}(x) = L_f T_i(x) = L_f^i h(x), \quad i = 1, 2, \dots, n-1$$

set of partial differential equations are

$$L_g L_f^{i-1} h(x) = 0; \quad i = 1, 2, \dots, n-1 \quad (6.6)$$

and also satisfy

$$L_g L_f^{i-1} h(x) \neq 0;$$

The main question is whether there exists  $h(x)$  that satisfies the equation (6.8). The given set of partial differential equations have a solution if the system is completely integrable. Frobenius

Theorem states that a distribution is completely integrable if and only if involutive [4].

A distribution  $\Delta$  is involutive if  $[f, g] \in \Delta$  whenever  $f, g \in \Delta$

**Theorem 2** The nonlinear system described by (6.1) is feedback linearizable if and only there is domain  $D_0 \subset D$  such that

1. The matrix  $\varsigma(x) = [g(x), ad_f g(x), \dots, ad_f^{n-1} g(x)]$  has rank  $n$  for all  $x \in D_0$
2. The distribution  $D = span\{g(x), ad_f g(x), \dots, ad_f^{n-2} g(x)\}$  is involutive in  $D_0$  [5].

### Full state feedback linearization for nonlinear systems

If the given nonlinear system satisfies above theorem we can calculate  $T, \alpha(x), \beta(x)$ . Then feedback linearized control design can be visualized as shown below

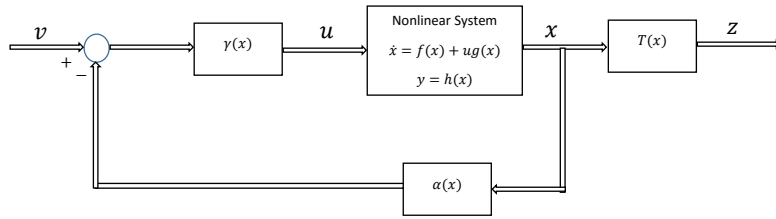


Figure 6.1: Feedback linearization

As  $v, z$  are related by the linear system equation given above, control design is straight-forward. The linear controller can then be used find  $u$  from the relation between  $u$  and  $v$  mentioned above.

## 6.2 Full state feedback linearization controller design for SOFC

The aim of the current study is to design a full state feedback linearized controller to control pressure dynamics, whenever there is a change in set point. Fluctuations in pressure dynamics decrease the life time of cell materials and also lead to variations in output voltage. We use the two input variables, fuel flow rate and air flow rate to control the partial pressure of water and partial pressure of oxygen respectively. Applying the procedure mentioned above for anode side and cathode side we can calculate  $T, \alpha(x), \beta(x)$  for fuel side and air side. The controller for the linear system is designed using pole placement. Finally, the feedback linearized controller is applied to the nonlinear system.

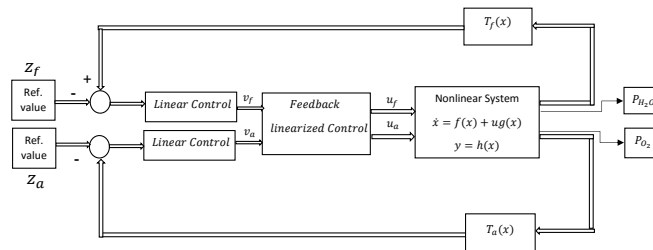


Figure 6.2: Feedback linearization controller



## 6.3 Results

After implementation of the full state feedback linearization control we observe that output responds faster to change in set point.

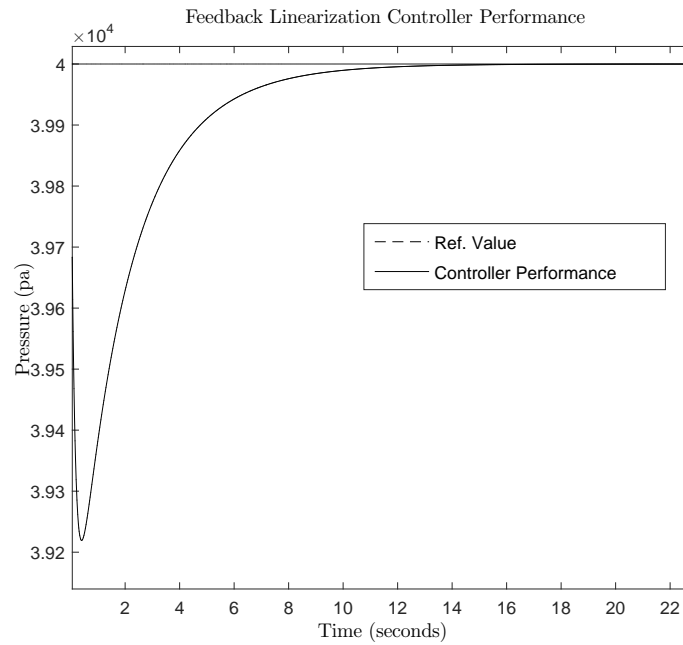


Figure 6.3: Feedback linearization controller for partial pressure of water set point  $4e4$  pa.

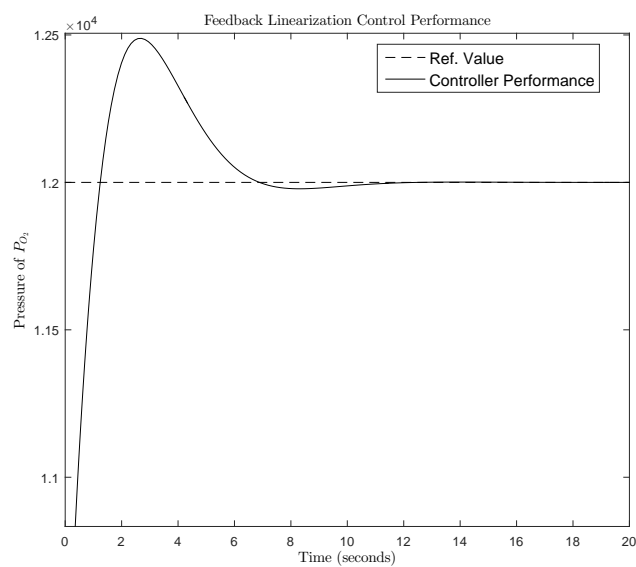


Figure 6.4: Feedback linearization controller for partial pressure of water set point  $1.2e4$  pa.

## 6.4 Comparison Between Feedback Linearization And Approximate Linearization Control Performance

We observe that full state feedback linearization control gives good control performance than control based on approximate linearization. When we give a step change in the desired output full state feedback linearization control gives good better performance.

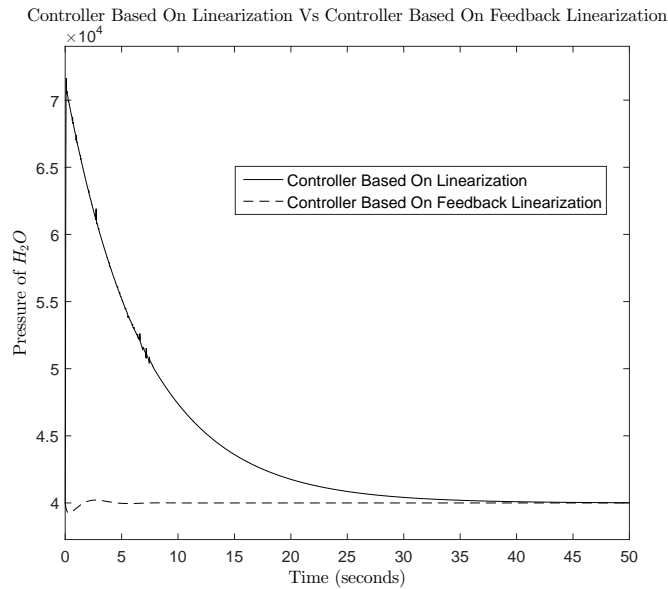


Figure 6.5: Ref. Pressure of  $H_2O$  is  $4e4$

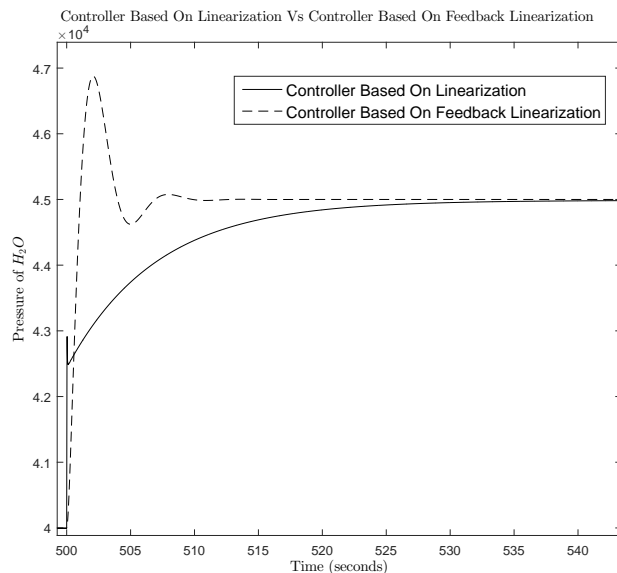


Figure 6.6: Step up in Ref. Pressure of  $H_2O$  from  $4e4$  to  $4.5e4$  pa.

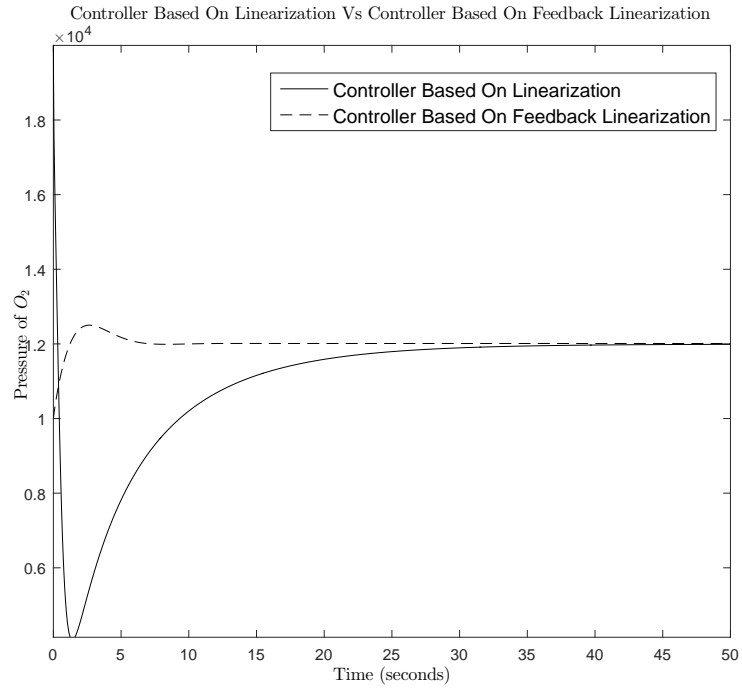


Figure 6.7: Ref. Pressure of  $O_2$  is  $1.2e4$  pa.

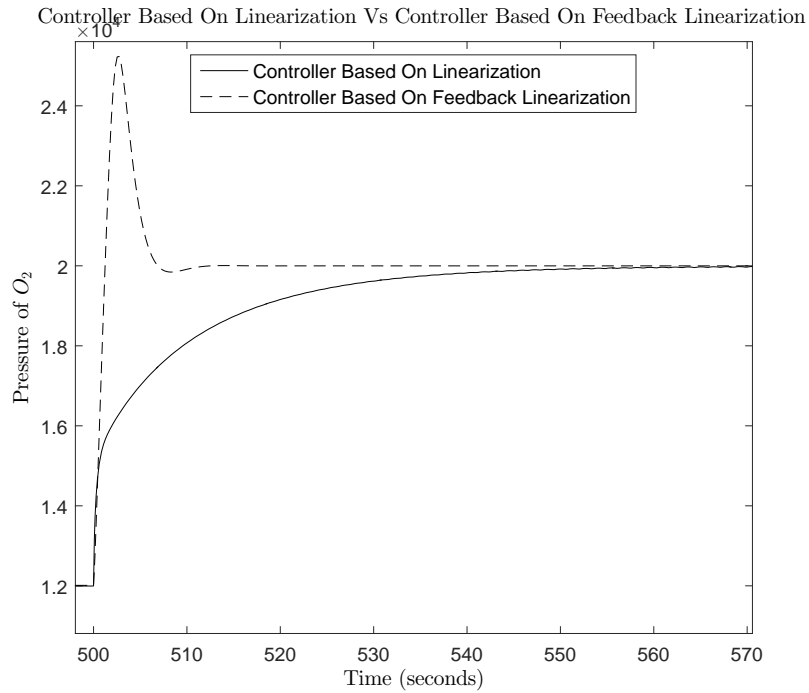


Figure 6.8: Step up in Ref. Pressure of  $O_2$  from  $1.2e4$  to  $2e4$  pa.

In the above figures we compare partial pressure dynamics of  $H_2O$  and  $O_2$  of full state feedback

linearize control and approximate linearization based control. Figure 6.5 shows the responses for partial pressure dynamics of  $H_2O$ . The output in the feedback linearization control reaches set point around 30 seconds faster than the approximate linearization based control. Figure 6.6 shows the output responses for set point change from  $4 * 10^4$  to  $4.5 * 10^4$ . Output of feedback linearized control reaches set point very fast with some overshoot. Figure 6.7 shows the output response for partial pressure dynamics of  $O_2$ . Again, the output from the feedback linearization control reaches set point around 30 seconds faster than approximate linearization based control. Figure 6.8 shows the output responses for set point change from  $1.2 * 10^4$  to  $2 * 10^4$ . If we use feedback linearization control, the set point is reached quickly with some overshoot.

## Chapter 7

# Conclusions And Future Work

**Modeling Of SOFC And Gain Scheduling** The results in chapter 3 indicate that proposed mathematical modeling of general SOFC produces results which are identical to the literature. This model exhibits traditional trends of all dynamic characteristics of output and state variables.

From the results in chapter 4 we can say that gain scheduling gives good control performance over the complete range of voltage for all operating points.

**Controllability And Observability** The results in chapter 5 indicate that if we can check the controllability and observability conditions we can then design a nonlinear controller and nonlinear estimator for SOFC.

**Feedback Linearization Controller** The results in chapter 6 indicates that feedback linearization controller gives good output responses than approximate linearization based controller. We highlight some challenges that need to be addressed.

- As Measuring component partial pressures of the SOFC is difficult, the states need to be estimated from input and output data?
- Input-output feedback linearization of the SOFC model is a challenging task. However, this gives the ability to directly control the voltage without requiring state estimators.
- Modification of feedback linearization controller to include noise, most of practical electrochemical device have noise.
- Development of a feedback linearization control for non-isothermal SOFC system, as the non-isothermal system is not of the form  $\dot{x} = f(x) + ug(x)$ .

# References

- [1] R. P. O’Hayre, S.-W. Cha, W. Colella, and F. B. Prinz. Fuel cell fundamentals, volume 2. John Wiley & Sons New York, 2006.
- [2] A. M. Murshed, B. Huang, and K. Nandakumar. Estimation and control of solid oxide fuel cell system. *Computers & chemical engineering* 34, (2010) 96–111.
- [3] R. Kandepu, L. Imsland, B. A. Foss, C. Stiller, B. Thorud, and O. Bolland. Modeling and control of a SOFC-GT-based autonomous power system. *Energy* 32, (2007) 406–417.
- [4] M. Vidyasagar. Nonlinear systems analysis, volume 42. Siam, 2002.
- [5] H. K. Khalil and J. Grizzle. Nonlinear systems, volume 3. Prentice hall New Jersey, 1996.
- [6] R. J. Braun. Optimal design and operation of solid oxide fuel cell systems for small-scale stationary applications. Ph.D. thesis, University of Wisconsin–Madison 2002.
- [7] A. M. Murshed, B. Huang, and K. Nandakumar. Control relevant modeling of planer solid oxide fuel cell system. *Journal of Power Sources* 163, (2007) 830–845.
- [8] V. M. Janardhanan and O. Deutschmann. Numerical study of mass and heat transport in solid-oxide fuel cells running on humidified methane. *Chemical Engineering Science* 62, (2007) 5473–5486.
- [9] J. Padulles, G. Ault, and J. McDonald. An integrated SOFC plant dynamic model for power systems simulation. *Journal of Power sources* 86, (2000) 495–500.
- [10] E. M. Fleming and I. A. Hiskens. Dynamics of a microgrid supplied by solid oxide fuel cells. In Bulk Power System Dynamics and Control-VII. Revitalizing Operational Reliability, 2007 iREP Symposium. IEEE, 2007 1–10.
- [11] K. Sedghisigarchi and A. Feliachi. Dynamic and transient analysis of power distribution systems with fuel Cells-part I: fuel-cell dynamic model. *IEEE transactions on energy conversion* 19, (2004) 423–428.
- [12] J. Blackburn and G. Reethof. Shearer. *JL, Fluid Power Control, Published joint by The Technology Press of MIT and John Wiley & Sons* .
- [13] R. H. Perry and D. W. Green. Perry’s chemical engineers’ handbook. McGraw-Hill Professional, 1999.

- [14] R. E. Kalman. Mathematical description of linear dynamical systems. *Journal of the Society for Industrial and Applied Mathematics, Series A: Control* 1, (1963) 152–192.
- [15] C.-T. Chen. Linear system theory and design. Oxford University Press, Inc., 1995.
- [16] R. Hermann and A. J. Krener. Nonlinear controllability and observability. *IEEE Transactions on automatic control* 22, (1977) 728–740.
- [17] W. K. Na and B. Gou. Feedback-linearization-based nonlinear control for PEM fuel cells. *IEEE Transactions on Energy Conversion* 23, (2008) 179–190.
- [18] L. J. Clancy. Aerodynamics. Halsted Press, 1975.
- [19] F. Lees. Lees’ Loss prevention in the process industries: Hazard identification, assessment and control. Butterworth-Heinemann, 2012.
- [20] J. Larminie, A. Dicks, and M. S. McDonald. Fuel cell systems explained, volume 2. Wiley New York, 2003.
- [21] F. Fahroo and I. M. Ross. DIDO (optimal control) .